https://doi.org/10.5194/egusphere-2026-5494
Preprint. Discussion started: 14 September 2026

Ammonia measurements over multiple fertilisation campaigns using eddy covariance and the integrated horizontal flux method

Sina Kukowski[1], Björn Kemmann[2,a], Pascal Wintjen[3], Paul Schmidt[4], Hans-Peter Piepho[4], Jeremy Rüffer[1], Jens-Kristian Jüdt[1], Melanie Saul[1], Hannah Götze[1,b], Andreas Pacholski[1], Heinz Flessa[1], Christian Brümmer[1]

[1]Thünen Institute of Climate-Smart Agriculture, 38116 Braunschweig, Germany
[2]Institute for Ecology, Chair of Soil Science, Technische Universität Berlin, 10587 Berlin, Germany
[3]Environmental Modelling, Sensing & Analysis, TNO, 1755LE Petten, The Netherlands
[4]Biostatistics Unit, Institute of Crop Science, University of Hohenheim, 70593 Stuttgart, Germany
[a]now at: Institute of Bio and Geo Sciences, Agrosphere (IBG-3), Forschungszentrum Jülich GmbH, 52428 Jülich, Germany
[b]now at: Institute for Biotechnology and Environmental Research, Faculty of Supply Engineering, Ostfalia University of Applied Sciences, 38302 Wolfenbüttel, Germany

Correspondence to: Sina Kukowski (sina.kukowski@thuenen.de)

Abstract. Quantifying field-scale ammonia emissions following nitrogen fertilisation remains challenging, and estimates may differ substantially between measurement methods. We compared quantum cascade laser-based eddy covariance (QCL-EC) with the integrated horizontal flux method using Adapted Low-cost Passive High Absorption (ALPHA) samplers (ALPHA-IHF) during eight urea fertilisation campaigns in winter wheat (2021–2023).

Both approaches identified post-fertilisation emission periods and captured similar dynamics, but paired interval estimates differed. Only 62% of intervals yielded ALPHA-IHF flux estimates, mainly because irregular or weak concentration profiles prevented robust calculation. QCL and ALPHA concentrations were positively correlated, but QCL concentrations were, on average, 31% higher, whereas QCL-EC emission estimates were 23% lower than ALPHA-IHF estimates. Median campaign emission factors were 1.6% for QCL-EC and 3.2% for ALPHA-IHF, respectively. QCL-based estimates were more precise, and differences between the methods varied with short-term ammonia concentration variability, air temperature, friction velocity and ALPHA profile quality.

The contrasting results show that concentration-level patterns do not translate directly into flux estimates and that differences between methods vary with field conditions. QCL-EC resolved short-term net exchange but required turbulence-based quality filtering, whereas ALPHA-IHF yielded time-integrated emission estimates only when the fitted concentration profile met the quality criteria. Without an independent reference, systematic over- or underestimation could not be assigned to either method. Assessments of fertiliser-induced emissions must consider method-specific data coverage and differences in flux representation. The greater precision of QCL-based estimates and high temporal resolution of QCL-EC make it promising for detecting subtle emission differences under low-emission conditions, while improved concentration precision and resolution of weak gradients could broaden ALPHA-IHF applicability.

https://doi.org/10.5194/egusphere-2026-5494
Preprint. Discussion started: 14 September 2026

1 Introduction

Atmospheric ammonia (NH_3) is a key transboundary air pollutant with significant implications for air quality, ecosystems, human health, and agricultural crop production. Through its reaction with other substances, NH_3 forms fine particulate matter ($PM_{2.5}$), a major contributor to health problems (Wyer et al., 2022). The nitrogen (N) deposition resulting from NH_3 emissions promotes eutrophication and poses a risk to natural and semi-natural ecosystems (Erisman et al., 2013; Sheppard et al., 2011). Additionally, NH_3 contributes to soil acidification, groundwater contamination, and the indirect formation of nitrous oxide (N_2O) through subsequent transformation processes, such as microbial oxidation in soils (Bremner, 1995; Canfield et al., 2010). In agricultural systems, NH_3 losses reduce the N-use efficiency of applied fertilisers (Liu et al., 2022; Govindasamy et al., 2023). Globally, agriculture accounts for approximately 81% of NH_3 emissions, highlighting the substantial scope for emission reductions within the sector (Wyer et al., 2022).

EU legislation, notably Directive (EU) 2016/2284 (the NEC Directive), requires reductions in national anthropogenic NH_3 emissions. Germany's reduction commitment is 29 % from 2030 onwards relative to 2005. For fertiliser application, emission factors (EFs), commonly expressed as the fraction of applied N emitted as NH_3-N, are key inputs to national emission inventories. However, the recommended EFs for urea have changed considerably in both magnitude and parameterization across successive editions of the EMEP/EEA guidebook, highlighting uncertainty in the selection of a representative EF for emission inventories (EMEP/EEA, 2009, 2013, 2016, 2023). Mineral N fertilisation, particularly with urea, has been estimated to account for 19.0–20.3 % of agricultural NH_3 emissions (Skorupka and Nosalewicz, 2021). The median NH_3-N emission factor for urea reported in the dataset underlying the IPCC (2019) methodology (14.2 %) and the EMEP/EEA (2023) urea EF (16.1 % for soils with pH ≤ 7) are higher than recent field-based estimates for (untreated) urea applied to winter wheat under German conditions, including a median of 4.8 % (mean: 8.5 %) reported by Kemmann et al. (2025) and a mean of 8.0 % reported by Frößl et al. (2026). These differences indicate that the representativeness of default EFs under these conditions warrants further evaluation.

Accurate NH_3 flux measurements are essential for refining EFs and mitigation strategies. Flux quantification relies on accurate NH_3 concentration measurements and appropriate methods for deriving the surface–atmosphere exchange. Techniques for concentration measurements commonly fall into passive samplers (e.g., ALPHA; Tang et al., 2001; Carozzi et al., 2013), optical real-time methods (e.g., quantum cascade laser absorption spectroscopy; Ellis et al., 2010; Whitehead et al., 2008; Wang et al., 2021), and wet chemistry systems (Erisman et al., 2001). These approaches also differ in whether NH_3 is measured directly in situ or collected before subsequent analysis. Passive samplers are low-cost and power-free but provide only time-integrated concentrations and the collected NH_3 must subsequently be extracted and analysed in the laboratory. They are also susceptible to contamination during preparation, handling and analysis. Optical methods provide direct in-situ measurements with high temporal resolution and can achieve sub-ppb sensitivity, but they are costly and require careful calibration and

https://doi.org/10.5194/egusphere-2026-5494
Preprint. Discussion started: 14 September 2026

maintenance. Wet-chemistry systems collect NH_3 in an aqueous absorbing solution, and the solution is either analysed automatically online, or subsequently in the laboratory. These systems can provide high sensitivity but require liquid reagents, pumps and regular maintenance. Regardless of the method, measuring atmospheric NH_3 concentrations remains challenging due to its adsorption and desorption on instrument surfaces, hygroscopic nature, high reactivity, low atmospheric concentrations, and pronounced spatial and temporal variability (Harper, 2005). Intercomparisons reveal biases up to 23 % and relative standard deviation of 10 to 50 % (Twigg et al., 2022; von Bobrutzki et al., 2010), especially at low ambient concentrations typical after synthetic fertiliser application.

Flux measurement approaches commonly include chambers (small-scale, intrusive) and micrometeorological techniques (field-scale, non-intrusive), each with specific limitations and challenges (e.g., Scotto di Perta et al., 2020). Among the latter, the integrated horizontal flux (IHF) method (Denmead, 1983) is widely used as a reference for fertiliser emissions, because it quantifies reliable field-scale fluxes under ambient conditions (Misselbrook et al., 2005; Yang et al., 2019; Götze et al., 2025; Sommer et al., 2005; Sommer and Misselbrook, 2016). IHF applications commonly employ wind-oriented Leuning passive flux samplers, which collect NH_3 in proportion to the product of wind speed and NH_3 concentration and therefore measure the time-integrated horizontal NH_3 flux at each sampling height (Leuning et al., 1985). Alternatively, active acid traps (e. g., Genermont et al., 1998) or passive diffusive concentration samplers, such as ALPHA samplers (e. g., Kemmann et al., 2025), can be deployed at several heights and combined with separately measured wind-speed profiles. Although IHF is a well-established micrometeorological reference approach, its implementation with ALPHA samplers is relatively recent. A direct comparison with established IHF measurements using Leuning samplers showed acceptable agreement, although some differences between the sampler–method combinations remained (Götze et al., 2025). The IHF approach has been criticised for overestimating NH_3 emissions (Sintermann et al., 2012) and is sensitive to assumptions about the concentration profile (Goedhart et al., 2020). The most direct approach for measuring large-scale trace gas exchange is eddy covariance (EC), which provides vertical fluxes without profile assumptions but requires NH_3 detection at a fast sample frequency and high precision. In recent years, considerable technological progress has been made in absorption spectroscopy, improving both measurement precision and the suitability of instruments for continuous field deployment. The use of quantum cascade lasers (QCL)-based absorption spectrometers in EC systems is therefore expected to yield more reliable estimates of NH_3 fluxes and their temporal dynamics (Zöll et al., 2016; Wang et al., 2022; Melman et al., 2026). Although QCL-based analyzers have previously been used for NH_3 flux measurements by EC (Ferrara et al., 2012; Moravek et al., 2019; Wang et al. 2021; Swart et al., 2023), direct field comparisons between QCL-EC and IHF-based emission estimates have not yet been reported.

The objective of this study was to evaluate the suitability and comparability of two approaches for quantifying NH_3 concentrations and emissions following repeated urea fertiliser applications under field conditions: QCL absorption spectroscopy within an eddy-covariance setup (hereafter QCL-EC) and ALPHA samplers combined with the integrated horizontal flux method (hereafter ALPHA-IHF). Specifically, we (i) compared NH_3 concentration and flux levels, temporal

https://doi.org/10.5194/egusphere-2026-5494
Preprint. Discussion started: 14 September 2026

emission dynamics, cumulative NH_3 emissions, and derived emission factors; (ii) evaluated overall agreement between paired measurements, including systematic differences, scatter among paired measurements, and the relative precision of the two approaches; and (iii) assessed whether agreement varied with methodological and environmental covariates and which covariates were most strongly associated with the observed discrepancies between the approaches.

2 Materials and methods

2.1 Site description and experimental setup

Experiments were conducted at conventionally managed winter wheat (*Triticum aestivum L.*, variety RGT Reform) fields over three consecutive years (2021–2023), from March to July each year. The measurement fields of approximately five hectares were located in central Germany, with the study site changing annually to maintain a representative crop rotation. All study sites were characterized by a temperate climate with a long-term mean annual temperature of 9.9 °C and mean annual precipitation of 616 mm (DWD, 2024).

The soil at the experimental sites was classified as a Stagnic/Orthic Luvisol according to the World Reference Base for Soil Resources (IUSS Working Group WRB, 2014). Soil texture corresponded to loam at the 2022 site (48.6 % sand, 37.3 % silt, 14.1 % clay) and to silt loam at the 2021 and 2023 site (17.6 % sand, 69.4 % silt, 13.0 % clay). The topsoils had a neutral pH (H_2O) of 7.1, a moderate soil organic-C content of 1.6 %, a cation-exchange capacity of 13 $cmol_c\ kg^{-1}$, and a urease activity of approximately 24 mg N $kg^{-1}\ h^{-1}$.

All fields were managed in accordance with local best management practices. Urea fertiliser was applied in three split applications each year, with single application rates ranging from 45 to 70 kg N ha^{-1}, resulting in a total N input of 155–170 kg N ha^{-1} per year. Calcium nitrate ($Ca(NO_3)_2$) fertiliser was applied to the surrounding buffer areas to ensure uniform crop growth in the surrounding field. After each fertiliser application, a measurement campaign (I, II, III) followed. Individual measurement campaigns lasted from six to 25 days depending on how long emissions remained elevated.

The experimental setup comprised a 140-metre-diameter circular source area (Fig. 1). This size was selected to balance the requirements of both the IHF, which typically requires a smaller radius, and the EC method, which benefits from a larger fetch. EC footprints were estimated in EddyPro using the Kljun et al. (2004) model and visually inspected in Tovi (LI-COR Environmental, Lincoln, NE, USA). The maximum contribution occurred at fetch distances of 26–29 m, and the mean (median) distance encompassing 90 % of the cumulative flux contribution was 53.1 m (48.0 m), indicating that the footprints were largely contained within the 70-m-radius experimental area. Occasional extensions reached only into the surrounding buffer zone.

https://doi.org/10.5194/egusphere-2026-5494
Preprint. Discussion started: 14 September 2026

The QCL inlet and all ALPHA samplers were positioned above the vegetation canopy throughout the measurement campaigns. ALPHA samplers were mounted at five heights and an EC tower equipped with a QCL positioned adjacent to it. Another IHF tower was positioned upwind in the $Ca(NO_3)_2$-fertilised area to capture background NH_3 concentrations. Horizontally homogeneous conditions were ensured, as no upwind obstacles were present that could influence atmospheric flow or measurement accuracy. Due to the extensive setup requirements, prohibitive costs, and workload, the full IHF–EC measurement setup was not spatially replicated at the site. Accordingly, the comparison is based on one paired measurement setup per campaign, with temporal replication provided by repeated measurements (once per day) throughout the emission period. Additionally, a weather station was installed within 100 meters of the measurement towers, and meteorological parameters, including precipitation, air temperature, relative humidity, and soil temperature, were recorded continuously during the measurement periods.

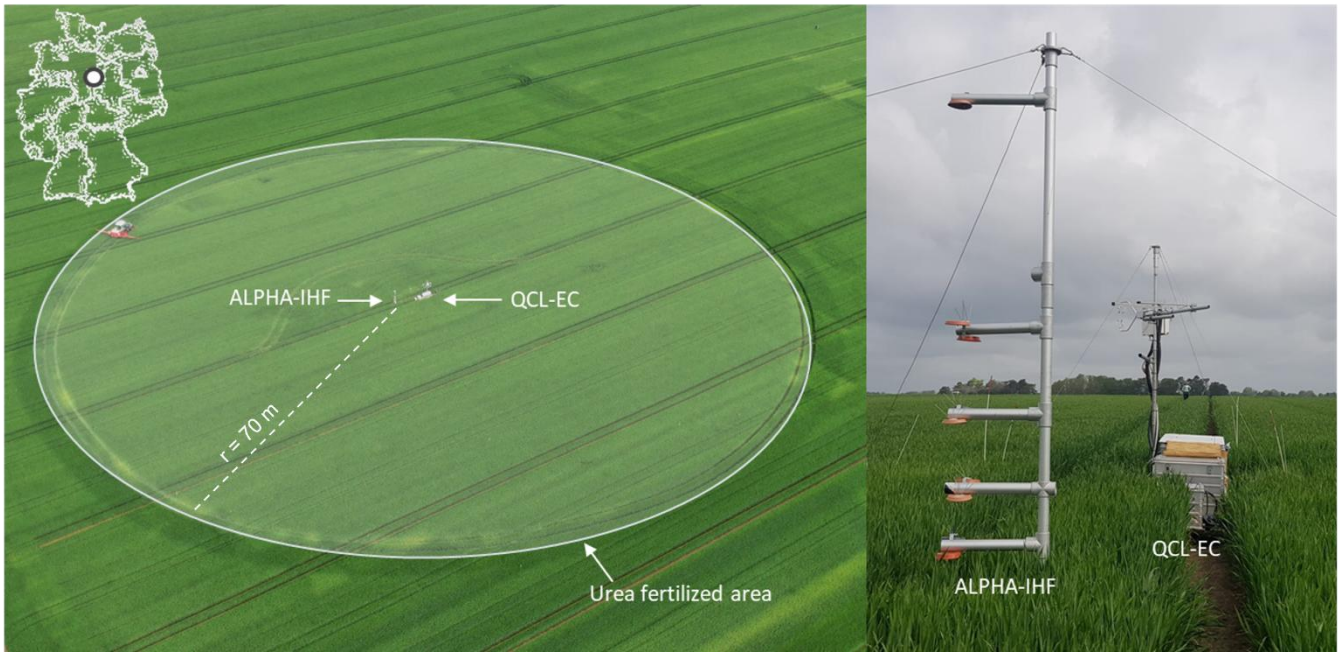

Figure 1: Experimental field setup and instrumentation for parallel NH_3 measurements using QCL-EC and the ALPHA-IHF in central Germany. The background sampling mast used for ALPHA-IHF was located outside the image frame.

2.2 QCL-EC method

2.2.1 Instrumentation in the field

An Aerodyne Research Inc. (MA, USA) Quantum Cascade Tunable Infrared Laser Differential Absorption Spectrometer (QC-TILDAS), here referred to as QCL, was used to measure NH_3 concentrations. The instrument was housed in a weatherproof box with active temperature control keeping diurnal amplitudes inside the housing <2 K to prevent instrumental drift. Air was sampled through the QCL inlet at a fixed height of 2.5 m above ground level (a.g.l.) through a quartz-siloxyl coated inertial inlet connected via a heated (40 °C) PFA sampling line (3.3 m). The sample air passes through a critical orifice, and

https://doi.org/10.5194/egusphere-2026-5494
Preprint. Discussion started: 14 September 2026

particles > 300 nm are removed via a 180° turn and pressure drop (~40 Torr). Air was drawn at ~15 sLpm by a dry scroll pump (TriScroll 600, Agilent Technologies, USA).

To minimize wall adsorption of NH_3 molecules, so-called active passivation was applied continuously by adding a fluorinated amine (perfluorotripentylamine), preventing NH_3 from adhering to the sample line or other internal surfaces as described by Roscioli et al. (2015). The glass inlet parts were cleaned before each campaign and, if necessary, during field operation.

NH_3 mixing ratios were measured at a frequency of 10 Hz in a 0.5 L multi-pass adsorption cell (76 m optical path). The QCL's detection limit is in the sub-ppb range (McManus et al., 2008). Internal system calibration was verified against HITRAN database absorption lines (Rothman et al., 2009). Further technical details and performance assessments of the QCL are reported by Zahniser et al. (2005), Ellis et al. (2010), and Zöll et al. (2016).

The QCL inlet was co-located with a 3-D sonic anemometer (CSAT3B, Campbell Sci., Logan, UT) for simultaneous turbulence measurements. The setup ensured unobstructed airflow for the prevailing westerly winds. The sonic anemometer recorded temperature and the three wind components (u, v, w) at 10 Hz. Wind speed, wind direction, friction velocity (u_*), and atmospheric stability parameters were derived from the anemometer data.

2.2.2 Data processing

Raw data processing and half-hourly flux calculations were performed using EddyPro 7.0.9 software (LI-COR Inc., 2011-2021). In addition to sonic anemometer and QCL data, external biometeorological variables – air temperature, atmospheric pressure, and relative humidity – were obtained from the nearby DWD (German Meteorological Service) weather station in Braunschweig. Dynamic meta data files were used, allowing canopy growth effects (see also section 2.3.1).

Data affected by instrument maintenance or poor performance were excluded after manual inspection. Since the coordinate system of the sonic anemometer must be aligned to the local wind flow, tilt correction was done by applying the double-rotation method (Wilczak et al., 2001). Turbulent fluctuations were extracted from the time-series data using block averaging as the detrending method. Time lags between the NH_3 concentration and vertical wind velocity signals, arising from transport through the inlet and sampling line and from the physical separation between the gas inlet and sonic anemometer, were determined and corrected using covariance maximization with default settings (minimum, nominal, and maximum time lag of 0 s, 1 s, 3 s, respectively). The mean time lag was 1.3 s, with a standard deviation of 0.79 s. Raw data despiking was performed following (Vickers and Mahrt, 1997).

High-frequency damping correction factors for NH_3 were determined for every half hour using the co-spectral method of Wintjen et al. (2020). This method uses the measured co-spectra of sensible heat (Co(w,T)) and NH_3 flux (Co(w,NH_3)) and

https://doi.org/10.5194/egusphere-2026-5494
Preprint. Discussion started: 14 September 2026

applies an empirical transfer function. A detailed description of the method can be found in Wintjen et al. (2020). Weekly mean damping factors were computed from half-hourly values and were applied to flux data. On average, the damping factor was 0.57, corresponding to a NH_3 flux loss of 43 % (range from 29 % to 53 %).

Quality control followed Mauder and Foken (2006), excluding fluxes if assigned a quality flag of 2. Fluxes associated with very stable atmospheric conditions ($u_* < 0.1$ m s^{-1}, cf. Zöll et al., 2016; Brümmer et al., 2022) were also excluded from further analysis.

For gap filling, we used the algorithm by Irvin et al. (2021) with minor adjustments for the NH_3 and the FluxGapfill python toolkit (Version 0.2.0; Irvin et al. (2021); https://github.com/stanfordmlgroup/methane-gapfill-ml, last access date: 15 July 2026). The input variables (predictors) were NH_3 concentration, air temperature, vapour pressure deficit, wind speed, wind direction, and relative humidity. Any gaps of less than six hours in the input variables were interpolated linearly beforehand. Larger gaps were not filled. The only exception was in 2021-III, where relative humidity and vapour pressure deficit showed a gap of 86.5 h which was filled using data from the weather station in the field. Gap-filling was done using gradient boosted regression trees (XGBoost). The dataset was split into a training and test dataset. Artificial gaps of different lengths were generated to train the model. Ten gap-filled flux scenarios are provided and an ensemble average is calculated as outcome. The uncertainty of the cumulative flux is calculated as the 1.96 standard deviation of the cumulative gap-filled flux scenarios.

2.3 ALPHA-IHF method

2.3.1 Profile measurements

Vertical profiles of NH_3 concentration $c(z)$, where z denotes the absolute height above ground level (a.g.l.), were measured using Adapted Low-cost Passive High-Absorption samplers (UKCEH ALPHA®, UK; Tang et al., 2001). ALPHA samplers are diffusion badge devices based on Fick's law of gas diffusion. A downward-facing PTFE membrane allows NH_3 to diffuse onto a citric acid-coated filter, which is sealed when not in use.

ALPHA samplers were mounted at five heights in the centre of the fertilised circular source area. The absolute sampling heights varied during the measurement campaigns and ranged from 0.3 to 3.2 m a.g.l., with all samplers positioned above the canopy. As the canopy developed, measurement heights were adjusted to remain above the canopy and to maintain the intended vertical distribution of the concentration profile. Each height was equipped with three replicate samplers protected by a rain shelter. The maximum sampling height was limited to 3.2 m a.g.l. for safety reasons. Background concentration c_B was determined upwind in the buffer area at three heights. Samplers were typically exposed for approximately 24 h (median: 24 h; IQR: 23–25 h, overall range 17–95 h). Longer exposures were used towards the end of the campaigns to ensure detectable concentrations during low NH_3 emission events.

https://doi.org/10.5194/egusphere-2026-5494
Preprint. Discussion started: 14 September 2026

After exposure, collected filters were extracted in 0.005 L deionized water, and the NH_4^+-N content of the extracts was quantified using an ammonia ion-selective electrode connected to a Versa Star Pro benchtop meter (Thermo Fisher Scientific, Waltham, MA, USA). Ion-selective electrode analysis has previously been validated for low-volume extracts from passive NH_3 samplers (Kure et al., 2020) and been used in several studies (e. g. Kemmann et al., 2025; Frößl et al., 2025a, 2026; Götze et al., 2025). The measured NH_3 mass, corrected for blanks, was converted to an average atmospheric concentration c (µg NH_3–N m^{-3}) using:

$$c = \frac{m}{V * t} \quad (1)$$

where m is the collected NH_3 mass (µg N), V the diffusive sampling rate (m^3 h^{-1}), and t the exposure time (h). According to Fick's law, the theoretical diffusive sampling rate is given by:

$$V = \frac{D * A}{L} \quad (2)$$

where D is the diffusion coefficient of NH_3 at 20 °C (m^2 h^{-1}), A = 3.4636 ×10^{-4} m^2 the cross-sectional area of the sampler, and L = 0.006 m the diffusion path length (Tang et al., 2001). For the concentration calculations, a membrane-specific diffusive sampling rate of 0.0035891 m^3 h^{-1}, as recommended by the UK Centre for Ecology & Hydrology (2021), was used. Triplicate NH_3 concentrations were averaged at each height, and the resulting five height-specific mean concentrations and their corresponding heights were used to fit the vertical concentration profile.

Wind speed $u(z)$ measurements were obtained simultaneously at three heights (0.3-2 m) using 2-D anemometers (two cup anemometers at the lower measurement heights and one sonic anemometer at a constant height of 2 m). As canopy height increased, lower measurement levels were adjusted. Each wind speed profile was visually inspected to ensure agreement between the two anemometer types. Individual measurements at the lower heights that appeared to be outliers, for example during periods of low wind speeds when cup anemometers underestimated wind speed because of breakaway friction, were excluded from subsequent wind profile calculations.

2.3.2 Flux calculation

The IHF method estimates NH_3 fluxes (F, µg m^{-2} s^{-1}) from vertical profiles of NH_3 concentration ($c(z)$) and horizontal wind speed ($u(z)$) by integrating the background-corrected product of concentration and wind speed over height in the center of the circular source area:

https://doi.org/10.5194/egusphere-2026-5494
Preprint. Discussion started: 14 September 2026

$$F = \frac{1}{x}\left[\int_{d+z_0}^{z_p} [c(z) - c_B]\, u(z)\, dz\right] \quad (3)$$

where x = 70 m is the fetch length of the source area to the sample mast, $d + z_0$ is the lower integration limit representing the zero-plane displacement height, and z_p is the upper integration limit. For numerical integration of the horizontal mass transport, $c(z)$ was parameterized using an exponential function and $u(z)$ using a logarithmic wind profile following Goedhart et al. (2020). Concentrations measured at the background mast (c_B) frequently exceeded those measured within the fertilised circular source area, and were therefore considered unsuitable for background correction. Consequently, and for consistency, c_B was derived from the α coefficient of the exponential $c(z)$ function, which represents the asymptotic concentration of the fitted concentration profile, and was used for background correction (Goedhart et al., 2020; Kemmann et al., 2025). Furthermore, the upper integration limit z_p was progressively restricted under conditions of increasing wind speeds and elevated c_B to account for increasing uncertainty in background concentrations estimates, as described in Kemmann et al. (2025). Surface roughness length z_0 and displacement height d were adjusted to account for canopy growth following Oke (1987) as implemented by Kemmann et al. (2025).

NH_3 fluxes were corrected for unaccounted turbulent transport (Wilson & Shum, 1992; Häni et al., 2016). Correction factors increased with z_0: 1.04, 1.08, 1.12 for campaigns I, II, III, respectively.

All concentration and wind profiles were checked individually for plausibility and consistency with the assumptions of the IHF approach. Intervals for which the profiles did not permit a valid IHF emission estimate, including inverse concentration profiles, were excluded from further emission calculations and coded as missing values (NA). No gap filling was applied. Cumulative IHF emissions were calculated from valid estimates only. Exposure period-specific comparisons between QCL-EC and ALPHA-IHF were restricted to paired observations for which valid emission estimates were available from both methods.

2.4 Data alignment and further calculations

QCL(–EC) measurements were conducted continuously from March to July each year. For method comparisons, only periods with concurrent ALPHA(–IHF) and QCL(–EC) data were considered. Each ALPHA exposure period and the corresponding temporally matched QCL(–EC) data defined a paired exposure period.

For the concentration comparison, the ALPHA concentration at 2.5 m a.g.l. was estimated for each paired exposure period by interpolation from the fitted exponential concentration profile, which was based on five height-specific triplicate means. Although 2.5 m was not a fixed ALPHA sampling height, it was within the vertical range covered by the samplers during all paired exposure periods. Profile R^2 was used as an indicator of fit quality. QCL mixing ratios measured directly at 2.5 m a.g.l. were converted from ppb to µg NH_3–N m^{-3} and averaged over the same paired exposure periods. The paired concentrations

https://doi.org/10.5194/egusphere-2026-5494
Preprint. Discussion started: 14 September 2026

thus represented the same absolute height and time period, but differed in that the QCL value was measured directly, whereas the ALPHA value was derived from the fitted profile.

For both methods, flux estimates were integrated over each paired exposure period to obtain exposure-period emissions (kg N ha^{-1}). Cumulative NH_3 losses and the corresponding emission factors were calculated for each campaign and year, with emission factors expressed as a percentage of applied N.

Selected meteorological variables (air temperature, relative humidity, vapour pressure deficit, wind speed, and friction velocity) were averaged over each paired exposure period and used as covariates in the statistical analysis. This aggregation matched the temporal resolution of the concentration and emission comparisons. The resulting covariate values therefore represent mean conditions during each paired exposure period rather than within-period variability.

2.5 Statistical analysis

All statistical analyses were performed using R (version 4.1.2; R Core Team, 2021). The general statistical procedure was applied separately to two endpoints: (i) NH_3 concentrations and (ii) NH_3 emissions.

As an initial comparison, simple linear regression analyses were performed, relating measurements obtained by one method (x) to the corresponding measurements obtained by the other method (y), and R^2 values and Pearson correlation coefficients were calculated.

These analyses describe association and linear calibration between methods, but they do not directly quantify the direction, magnitude and variability of paired method differences. Therefore, Bland-Altman analysis (Bland and Altman, 1999) was used to assess systematic method differences across the observed measurement range. For each paired observation, the difference between the two methods was calculated and plotted against their mean. The standard Bland-Altman plot revealed heteroscedasticity, with a funnel-shaped scatter for both the concentration and emission data. This was addressed by switching to a log scale, which linearised proportional relationships and considers ratios rather than absolute differences. On the log scale, a systematic trend remained in both datasets. This apparent trend was, however, attributed to method-specific variance heterogeneity, based on the estimated variances of and covariance between the two methods obtained via a bivariate model (see supplements). This was then addressed by using a precision-weighted mean (w) instead of the simple arithmetic mean. In this weighted mean, the more precise method contributes more strongly to the estimate of the measurement level. The bias, the standard deviation of the log differences, and the Limits of Agreement (LoAs) were calculated.

In the next step, covariates were selected in two stages, to investigate the factors associated with the differences between the two methods. First, candidate variables were chosen based on their expected mechanistic relevance to NH_3 measurements. Second, pairs of highly correlated variables ($r > 0.7$) were identified, and within each such pair, the variable with stronger theoretical relevance (more directly related to the expected underlying process) was retained to reduce multicollinearity. With the selected covariates, linear regression models were fitted using log(QCL/ALPHA) for concentrations and log(QCL-EC/ALPHA-IHF) for emissions as response variables. Three linear models were compared: one with the measurement level as the only predictor, one with covariates only as predictors, and one with a combination of both. In contrast to the Bland-

https://doi.org/10.5194/egusphere-2026-5494
Preprint. Discussion started: 14 September 2026

Altman analysis above, these models used the unweighted mean of the log-transformed measurements as a proxy for the measurement level. The precision-weighted mean w was not used as a covariate here, because by construction w satisfies cov(d, w) = 0, and would therefore not capture measurement-level trends that should be controlled for when assessing additional covariate effects.

Explained variance (R^2) was calculated for each model, and F-tests were used to assess whether adding covariates significantly improved the model fit. To compare covariate effect sizes, all covariates were Z-standardised, and exponentiated regression coefficients were calculated. Model-adjusted covariate effects were visualized using partial residual plots. These plots were used to illustrate the fitted effect of each covariate on the method ratio after adjustment for measurement level and the remaining covariates.

As a diagnostic extension of the Bland-Altman analyses, an extended bivariate model (adding method × covariate interactions) was fitted to estimate method-specific covariate slopes and residual variances, allowing to identify which method drove covariate-dependent differences in the method ratio and whether covariates explained part of the observed precision differences. A more detailed description of the statistical approach is provided in the supplements.

3 Results

To assess the agreement between the two measurement systems in quantifying atmospheric NH_3 concentrations, a total of 98 paired measurements from 8 fertilisation campaigns, each lasting between 8 and 20 days, were analysed (Table 1). Due to missing or unreliable ALPHA data, 12 data pairs in 2021 had to be excluded from the concentration analysis leading to a remaining sample size of n = 86 pairs. The observed values covered a concentration range of 0.1 to 39.6 µg NH_3 m^{-3}. Overall, the median NH_3 concentrations measured by the two systems agreed reasonably well, suggesting that both methods captured similar concentration levels (Table 2).

Across both methods and all paired exposure periods, exposure-period emissions ranged from 0.002 to 1.238 kg N ha^{-1}, with campaign-specific medians ranging from 0.01 to 0.30 kg N ha^{-1}. In 38 % of the cases, no ALPHA-IHF emissions could be determined from the profiles. These data points were excluded from further analysis, leaving a sample size of n = 59 for further emission analysis.

Table 1: Overview of campaign characteristics and meteorological conditions. T_a = average air temperature, RH = average relative humidity, WS = average wind speed.

Campaign	Fertiliser N applied kg N ha^{-1}	Duration of campaign days	T_a (°C)	RH %	WS m s^{-1}
2021-II	70	8	9.49	69.08	3.00
2021-III	60	13	14.68	77.38	2.12
2022-I	45	16	7.54	65.66	2.56
2022-II	60	14	10.40	68.48	1.95

https://doi.org/10.5194/egusphere-2026-5494
Preprint. Discussion started: 14 September 2026

Campaign	Fertiliser N applied kg N ha^{-1}	Duration of campaign days	T_a (°C)	RH %	WS m s^{-1}
2022-III	50	11	15.67	69.88	2.37
2023-I	60	14	8.66	75.33	3.56
2023-II	50	14	10.41	65.77	2.87
2023-III	45	20	16.09	61.89	1.68

340 **Table 2: Overview of campaign-level NH_3 concentrations and emissions. Values are presented as medians [25th–75th percentiles]. n_{conc} denotes the number of paired exposure intervals available for the concentration comparison, and n_{em} the number of paired intervals with valid emission estimates for both methods. Missing ALPHA-IHF estimates indicate the percentage of ALPHA exposure intervals for which no valid flux estimate could be derived.[1]**

Campaign	n_{conc}	NH_3 concentration ALPHA at 2.5 m a.g.l (profile-derived) µg m^{-3}	NH_3 concentration QCL at 2.5 m a.g.l. µg m^{-3}	n_{em}	NH_3 emission QCL-EC kg N ha^{-1}	NH_3 emission ALPHA-IHF kg N ha^{-1}	Missing ALPHA-IHF estimates %
2021-II	3	3.4 [3.1–5.8]	4.2 [3.5–4.7]	3	0.03 [0.0–0.0]	0.15 [0.1–0.2]	40
2021-III	3	2.8 [2.0–3.1]	1.8 [1.4–2.2]	2	0.01 [0.0–0.0]	0.01 [0.0–0.0]	80
2022-I	15	13.3 [11.8–25.4]	16.3 [13.3–18.5]	12	0.16 [0.1–0.2]	0.13 [0.1–0.8]	20
2022-II	14	3.2 [2.1–6.5]	6.3 [5.4–9.4]	12	0.06 [0.0–0.2]	0.11 [0.0–0.2]	14
2022-III	7	3.5 [2.1–5.1]	9.0 [4.9–9.9]	6	0.12 [0.0–0.2]	0.04 [0.0–0.2]	14
2023-I	12	9.5 [3.5–11.2]	7.8 [5.9–9.8]	8	0.08 [0.0–0.1]	0.30 [0.1–0.6]	33
2023-II	14	4.2 [2.6–7.0]	4.2 [3.6–6.0]	7	0.05 [0.0–0.2]	0.14 [0.1–0.2]	50
2023-III	18	3.4 [1.7–11.5]	3.9 [3.1–6.5]	9	0.03 [0.0–0.1]	0.07 [0.0–0.2]	50

[1] Emission values are unweighted medians of exposure-period emissions and are not normalized by exposure period or campaign duration. Campaign duration and cumulative emissions are reported separately in Table 1 and Table 3.

https://doi.org/10.5194/egusphere-2026-5494
Preprint. Discussion started: 14 September 2026

3.1 Time series

Figure 2 illustrates the temporal patterns of the concentration and emission data. The time series shows that both methods capture the same fundamental patterns in terms of concentrations as well as emissions. Increases and decreases run largely in parallel, suggesting basic similarities in emission process observation. During parts of Campaign I in 2022 and Campaigns II and III in 2023, ALPHA-IHF yielded markedly higher emission estimates and more pronounced temporal peaks than QCL-EC. Numerous missing values in the ALPHA-IHF data (displayed as “x”) are striking. However, most of the missing IHF estimates occurred toward the end of the campaigns under very low-emission conditions (Fig. 2b).

https://doi.org/10.5194/egusphere-2026-5494
Preprint. Discussion started: 14 September 2026

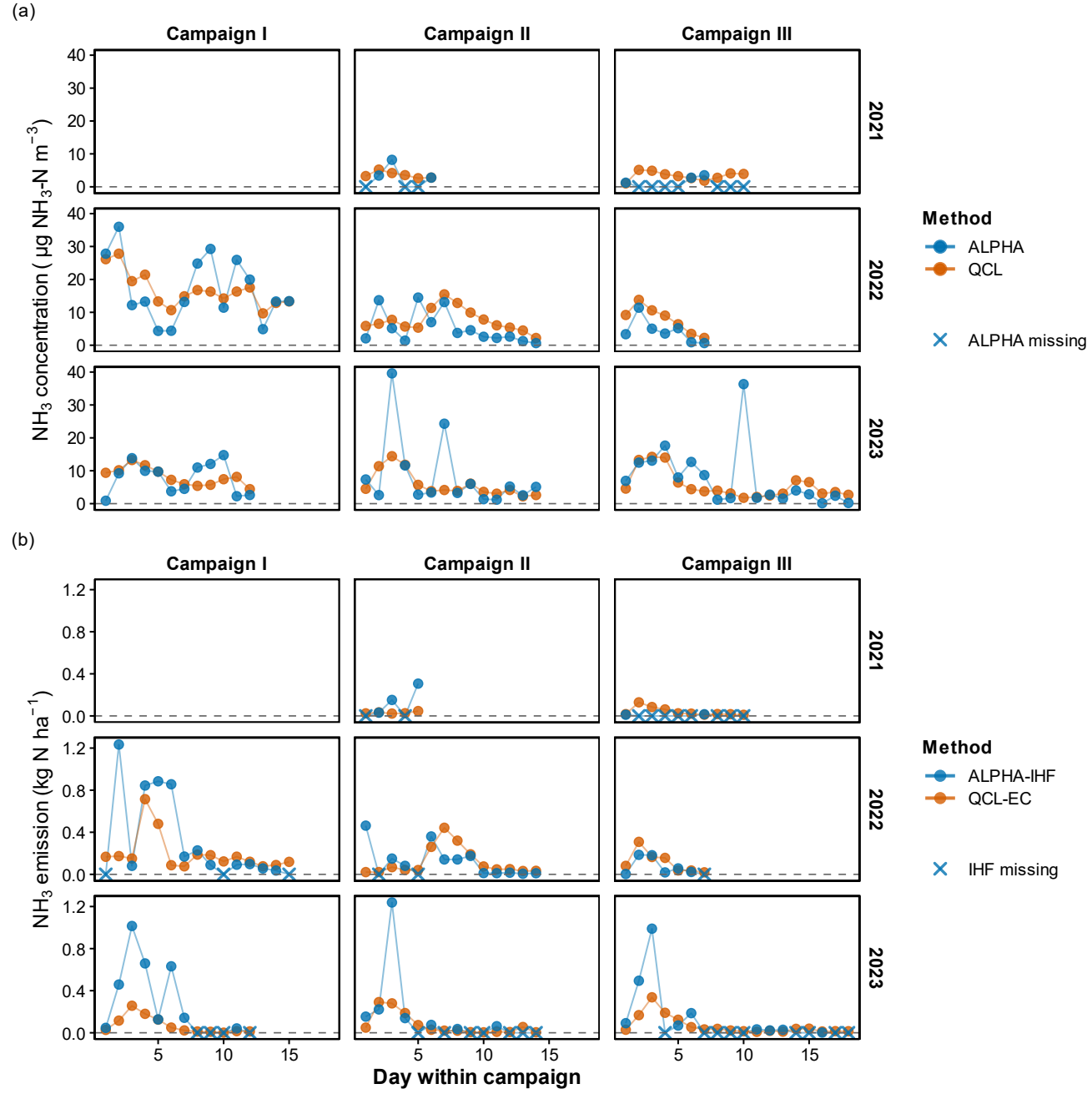

Figure 2: Time series of NH_3 concentrations (a) and emissions (b) obtained during different campaigns (columns) and years (rows). Each point represents the mean concentration or integrated emission over the corresponding ALPHA exposure period. QCL concentrations were averaged and QCL-EC fluxes integrated over the same exposure periods. Lines connect consecutive exposure periods for each method.

https://doi.org/10.5194/egusphere-2026-5494
Preprint. Discussion started: 14 September 2026

High-temporal-resolution eddy covariance measurements (Fig. 3) provide insight into the highly dynamic nature of NH_3 emissions after fertiliser application over time. Considering all measurement campaigns over the three years, the first peak emission occurred on average after 2.3 days (an exception is campaign II-2022), and elevated emission levels were observed for on average 2.7 days before the decline started. Peak timing and onset of decline were derived from 6-h mean QCL-EC flux time series. The first relevant peak was defined as the first local maximum reaching at least 70 % of the campaign maximum, and the onset of decline as the first sustained decrease lasting at least 48 h. The highest flux was measured on April 26, 2022 at 8:30 p.m. (Campaign II), at 3655 ng NH_3-N m^{-2} s^{-1} (six days after fertiliser application and just after a 3.6 mm rain event). Across all campaigns, 85.7 % of cumulative NH_3 emissions occurred within the first seven days after fertilisation (median, range 56.3–96.2 %). NH_3 fluxes generally followed a diurnal pattern when grouped by hour of the day across campaigns, with maxima around noon and minima at night-time. NH_3 concentrations, however, did not show clear diurnal patterns, when averaged by hour of day, but rather high fluctuation.

https://doi.org/10.5194/egusphere-2026-5494
Preprint. Discussion started: 14 September 2026

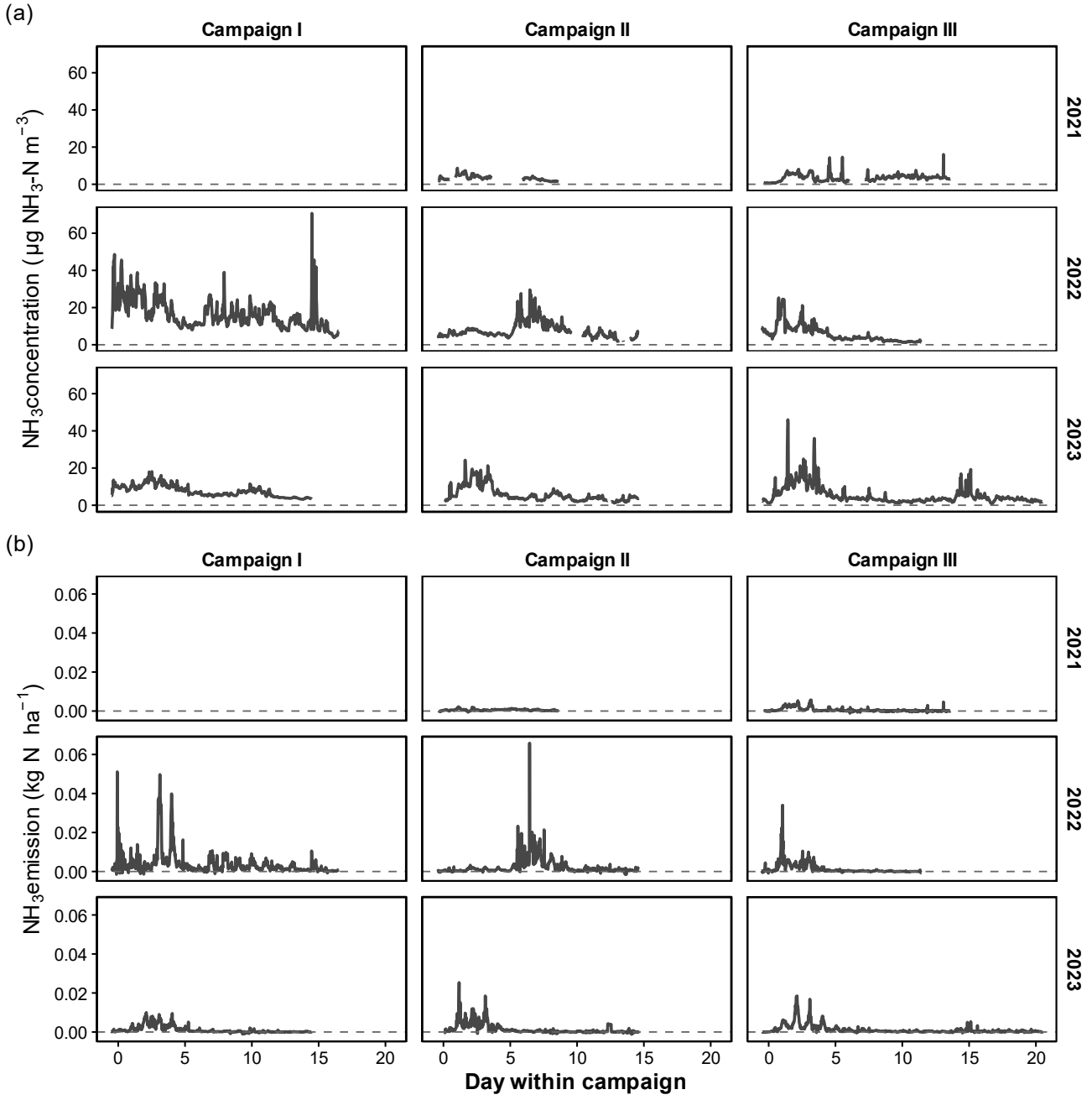

Figure 3: Time series of half-hourly mean NH_3 concentrations measured by the QCL (a) and half-hourly integrated NH_3–N emissions derived by QCL-EC (b) for the individual fertilisation campaigns from 2021 to 2023. Gaps in the QCL-EC emission time series were filled as described, whereas concentration data were not gap-filled. Breaks in the concentration time series indicate periods without valid QCL measurements.

https://doi.org/10.5194/egusphere-2026-5494
Preprint. Discussion started: 14 September 2026

3.2 Cumulative emissions

Table 3 shows the cumulative NH_3 emissions as a percentage and in kg N ha^{-1} during the different measurement periods, as determined by the QCL-EC and ALPHA-IHF methods. ALPHA-IHF emissions exceeded QCL-EC losses in most campaigns. Overall, the median difference in cumulative losses between the two methods is 0.72 kg N ha^{-1} (mean = 0.84 kg N ha^{-1}), ranging from -2.33 to +0.32 kg N ha^{-1} depending on the measurement campaign. On average, emissions are approximately twice as high with the ALPHA-IHF method, resulting in a median emission factor of 3.2 % (mean 3.5 %), compared to 1.6 % (mean 1.8 %) of applied N with the QCL-EC method. Two campaigns show slightly higher losses observed with the QCL-EC method (2022-II and 2022-III). These two campaigns both show generally very low emissions. Additionally, in 2021, only a few data points were available for the comparison due to missing ALPHA-IHF values. Overall, regression analysis revealed a positive correlation between QCL-EC and ALPHA-IHF emissions, with a moderate to strong coefficient of determination (R^2 = 0.67).

Table 3: Cumulative NH_3 emission as the fraction of applied N in percentage and in kg N ha^{-1} during the different measurement periods measured with the QCL-EC and the ALPHA-IHF method. The durations of the campaigns are listed in Table 1.

Campaign	QCL-EC % $N_{applied}$	ALPHA-IHF % $N_{applied}$	QCL-EC kg N ha^{-1}	ALPHA-IHF kg N ha^{-1}	Difference (QCL-EC − ALPHA-IHF) kg N ha^{-1}
2021-II	0.15	0.70	0.10	0.49	-0.39
2021-III	0.05	0.04	0.03	0.03	0.00
2022-I	5.56	10.37	2.50	4.67	-2.16
2022-II	2.64	2.61	1.58	1.57	0.02
2022-III	1.57	0.94	0.78	0.47	0.32
2023-I	1.32	5.20	0.79	3.12	-2.33
2023-II	1.73	3.85	0.86	1.93	-1.06
2023-III	1.69	4.26	0.76	1.92	-1.15
Mean	1.84	3.50	0.93	1.77	-0.84
Median	1.63	3.23	0.79	1.74	-0.72

3.3 Regression and Bland-Altman analysis

For the initial linear regression analyses, the method placed on the x-axis differed between comparisons. QCL was used for the concentration comparison because it provided a direct measurement at the comparison height, whereas the corresponding ALPHA concentration was derived from the fitted vertical profile. For the emission comparison, ALPHA-IHF was used as a pragmatic reference because IHF approaches have been more widely validated. These choices do not imply that either method represents an absolute benchmark, as both remain subject to uncertainty.

https://doi.org/10.5194/egusphere-2026-5494
Preprint. Discussion started: 14 September 2026

Figure 4a shows a clear positive relationship between QCL and ALPHA-derived concentrations, although considerable scatter remained (Pearson r = 0.62, p < 0.001). The slope of approximately 1 indicates that the concentrations changed proportionally, but does not imply close correspondence in absolute values.

Figure 4b shows the corresponding emission comparison and reveals a moderate positive correlation between the QCL-EC and ALPHA-IHF emission estimates (Pearson's r = 0.54, p < 0.001). QCL-EC emissions were generally lower than ALPHA-IHF emissions, the slope differed significantly from 1, and the linear model explained 30 % of the variance.

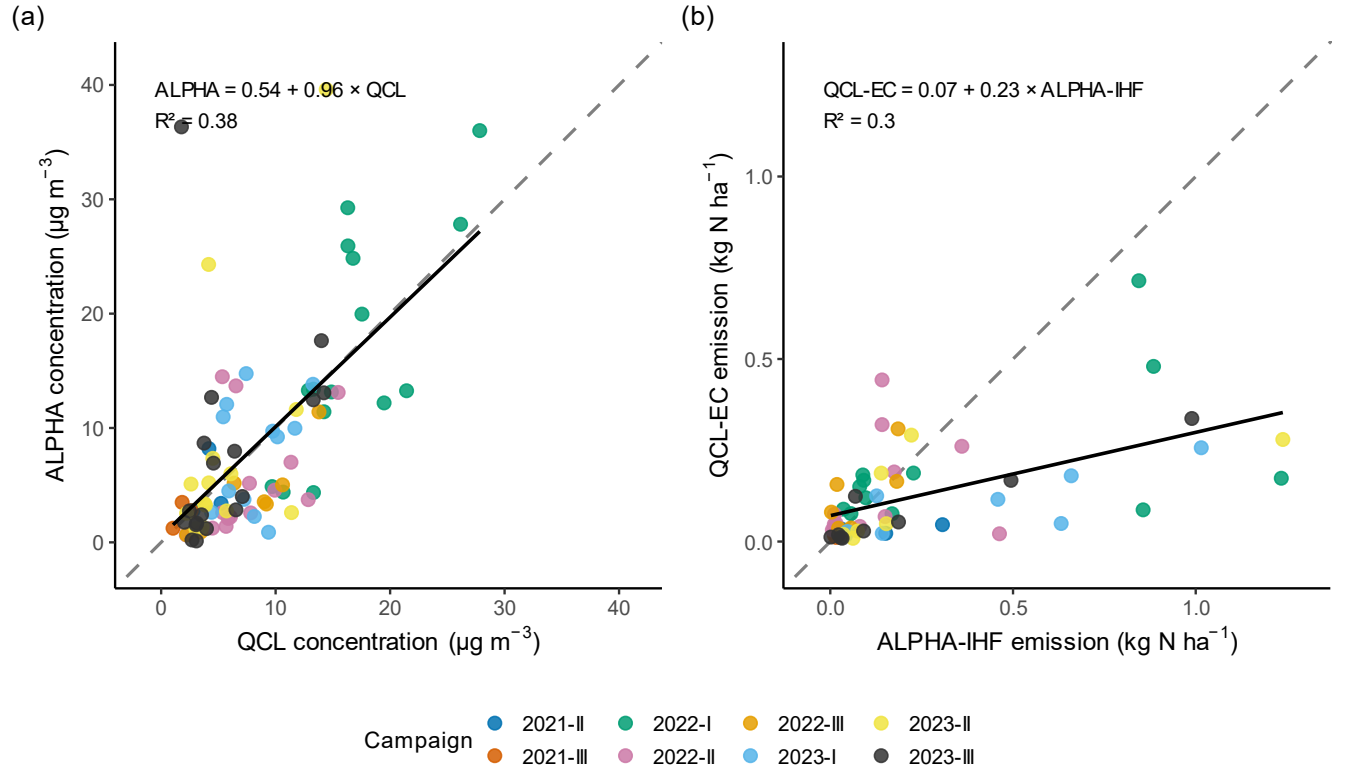

Figure 4: Comparison of NH_3 concentrations (a) and exposure-period NH_3 emissions (b) obtained using QCL(-EC) and ALPHA(-IHF) across all measurement campaigns (2021–2023). In panel (a), each point compares the mean QCL concentration over an ALPHA exposure period with the corresponding profile-derived ALPHA concentration at 2.5 m a.g.l. In panel (b), each point compares the QCL-EC and ALPHA-IHF emissions integrated over the same ALPHA exposure period. Points are colored by year and campaign. The dashed line represents perfect agreement (1:1), and the solid line shows the linear regression across all observations.

As previously mentioned, a Bland-Altman analysis was performed using a precision-weighted mean rather than a simple arithmetic mean to account for unequal precision in the methods, i.e., giving greater weight to the more precise QCL(-EC) measurements. The variances of and covariance between methods (see supplements) revealed differences in measurement precision (Table 4). The common variance component (τ^2 = 0.49 for concentrations and 1.02 for emissions) represents the

https://doi.org/10.5194/egusphere-2026-5494
Preprint. Discussion started: 14 September 2026

shared, method-independent variation between observations, whereas the method-specific error variances reflect additional measurement uncertainty for each method. For both concentrations and emissions, ALPHA(-IHF) showed the larger method-specific error SD (ratio 1.6 and 1.4 respectively), indicating lower precision than QCL(-EC).

Table 4: Variances, covariance, and precision estimates for the QCL(-EC) and ALPHA(-IHF) measurement systems.

Quantity	Meaning / interpretation	Concentration (n = 86)	Emission (n = 59)
σ (QCL)	Total observed standard deviation of QCL measurements, including shared signal and method-specific error	0.705	1.123
σ (ALPHA)	Total observed standard deviation of ALPHA measurements, including shared signal and method-specific error	1.130	1.542
ρ	Within-unit correlation between paired QCL and ALPHA measurements	0.612	0.587
a (QCL)	Relative weight of the QCL measurement in the precision-weighted mean	0.987	0.848
τ^2	Variance component representing the shared true signal between both methods	0.488	1.017
σ_e^2 (QCL)	Estimated method-specific error variance of QCL measurements	0.010	0.244
σ_e^2 (ALPHA)	Estimated method-specific error variance of ALPHA measurements	0.789	1.362

Figure 5 shows the differences between the two methods plotted against the precision-weighted mean of each pair of measurements. For the concentrations (Panel a), the observed bias (dashed line) is positive, indicating that the QCL method yields, on average, values that are 31 % higher than those of the ALPHA method (0.27 on a log scale). Five data points lie outside the LoAs, indicating cases where the methods disagree significantly. To illustrate the width of the LoAs: anchored at an ALPHA reading of 1 µg/m³, the corresponding QCL values would lie between 0.23 and 7.57 µg/m³ (LoA: 0.23 to 7.57); at 5 µg/m³ ALPHA, between 1.15 and 37.85 µg/m³. Equivalently, individual ratios at the LoA boundaries correspond to QCL being about 77 % below ALPHA at the lower limit and 657 % above at the upper limit.

The equivalent Bland-Altman plot for emissions (Panel b) shows that QCL-EC, on average, measures 23 % less than ALPHA-IHF. While most of the data points lie within LoAs, they cover a wide multiplicative range. On the log scale, the LoAs span approximately five log units, corresponding to a roughly 153-fold range on the original ratio scale (LoA: 0.06 to 9.18). At the LoA boundaries, individual ratios thus reach extremes of QCL-EC being approximately 94 % below and 818 % above ALPHA-IHF, respectively. This indicates high variability and potentially poor agreement.

https://doi.org/10.5194/egusphere-2026-5494
Preprint. Discussion started: 14 September 2026

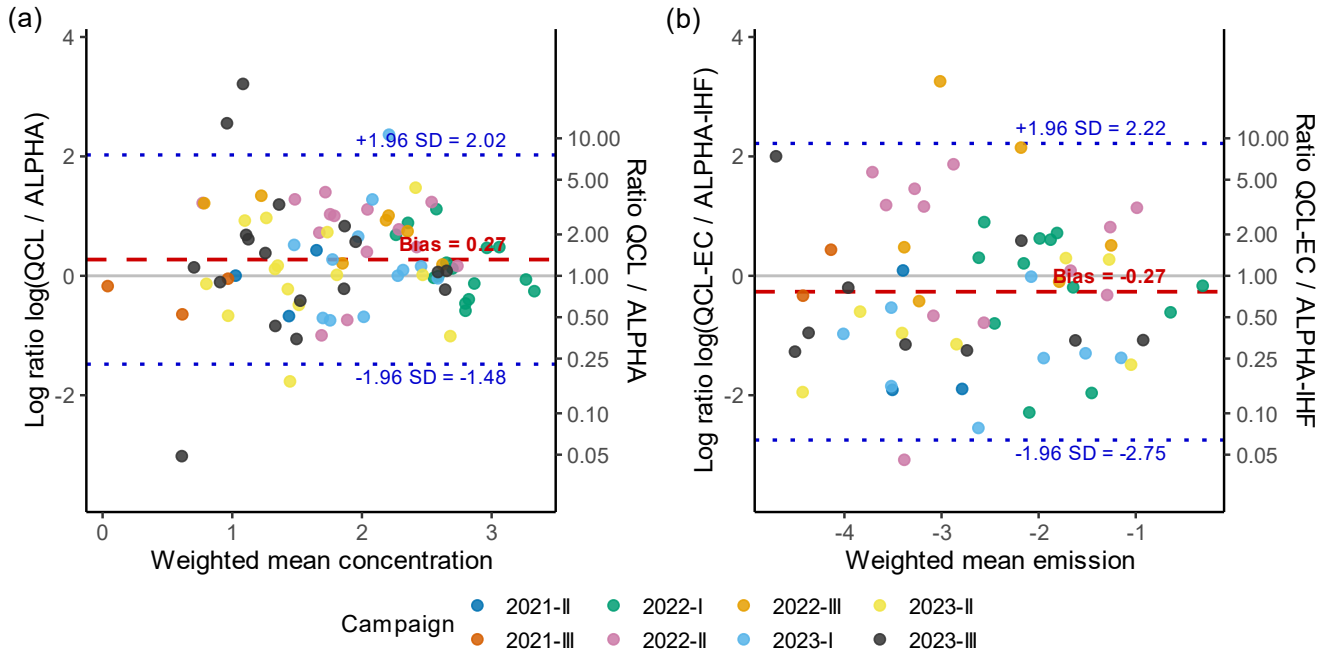

435 **Figure 5: Bland–Altman plots of the log-transformed ratios of QCL to ALPHA concentrations (a) and QCL-EC to ALPHA-IHF exposure-period emissions (b), plotted against the corresponding precision-weighted means. Each point represents a paired ALPHA exposure period, with QCL concentrations averaged and QCL-EC emissions integrated over that period. The dashed red line indicates the estimated mean bias, the dotted grey lines the limits of agreement (mean bias ± 1.96 SD), and the solid grey line zero difference (perfect agreement). The secondary y-axis shows the corresponding ratios on the original scale. Points are coloured by year and campaign.**

440 **3.4 Covariate Analysis**

While the results in 3.3 assessed the general level of agreement between the measurement methods, a key question in this study was whether this depends on environmental conditions. In other words, are there situations (such as specific turbulence conditions, temperature ranges, radiation or wetness regimes, etc.) in which the methods agree better than in other? The selected covariates comprise air temperature (T_a), relative humidity (RH), friction velocity (u_*), variability in atmospheric NH_3 445 concentration (QCL SD), and ALPHA profile quality (R^2 of fitted concentration profile curve, hereafter R^2 profile). The results of the covariate analysis are displayed in Table 5.

https://doi.org/10.5194/egusphere-2026-5494
Preprint. Discussion started: 14 September 2026

Table 5: Model comparison for concentration and emission log ratios based on explained variance and AIC. The unweighted mean of the log-transformed measurements was used as a proxy for the measurement level. The covariates are air temperature, relative humidity, friction velocity, variability in atmospheric NH_3 concentration, and ALPHA profile quality.

y-Variable	Model	R^2	adj. R^2	AIC
Concentrations Log(QCL/ALPHA)	(1) Measurement level	27.6 %	26.7 %	202.0
	(2) Covariates	6.8 %	0.9 %	231.7
	(3) Measurement level + Covariates	47.0 %	42.9 %	185.2
Emissions Log(QCL-EC/ALPHA-IHF)	(1) Measurement level	13.7 %	12.2 %	191.7
	(2) Covariates	44.9 %	39.7 %	173.2
	(3) Measurement level + Covariates	49.4 %	43.6 %	170.1

Regarding the concentrations, at first glance, the covariates appear to explain little (7 %) on their own. However, the picture changes when they are considered alongside the measurement level: the model improves from 28 % to 47 % – an increase of 19 percentage points (F-test: $p < 0.001$). Beyond the sole measurement level effect, the covariates explain a substantial proportion of the systematic variation in the method ratio. The most significant individual contribution comes from QCL SD (the variability of the NH_3 concentration determined by QCL within the exposure period), explaining 42 % of the variance. The ALPHA profile quality contributes with 32 % explained variance. The remaining covariates (u_*, T_a, RH) each explain 28 % of the variance.

For the emissions, covariates already explain almost 45 % of the variance. When the measurement level is considered in addition, the model improves by 4.5 percentage points in explained variance. Thus, the covariates alone explain a substantial proportion of the systematic variation in the emission ratio. The remaining ~ 55 % of unexplained variance reflects the inherent difficulty of comparing emissions using two different methods based on fundamentally different assumptions and are at the same time prone to measurement errors due to various reasons (e.g., contaminations in NH_3 concentration readings).

The effect sizes and statistical significance of the covariates, expressed as standardized regression coefficients (exponentiated), are visualized in Figure 6. Each coefficient represents the multiplicative change in the ratio between methods for a one-standard-deviation (1 SD) increase in the covariate, with 95 % confidence intervals shown as horizontal bars. Covariates with coefficients that differ significantly from 1 (indicated by the dashed line) are marked with asterisks (* $p < 0.05$, ** $p < 0.01$, *** $p < 0.001$).

Positive estimates (Fig. 6) mean that with an increase in this covariate, the ratio increases. The further interpretation can, however, cover several scenarios: the relationship may move towards 0 (i.e., better agreement, on a log scale) or further away from it (i.e., poorer agreement). For concentration differences, increasing diurnal NH_3 variability is associated with an increase

https://doi.org/10.5194/egusphere-2026-5494
Preprint. Discussion started: 14 September 2026

in the QCL-to-ALPHA ratio, indicating that QCL yields higher values relative to ALPHA under conditions of high variability. Thus, the bias between the methods depends on the magnitude of diurnal NH_3 variability. QCL SD showed a significant positive effect ($\beta = 0.219$, $\exp(\beta) = 1.245$, $p < 0.001$). A 1 SD increase in diurnal NH_3 variability is therefore associated with a 25 % increase in the relative difference between QCL and ALPHA. The quality of the ALPHA profile was also significant. By contrast, u_* was not statistically significant, indicating that there was no reliable association between the methods' relative differences.

For emission differences, the covariate with the highest significant effect size is the variability of atmospheric NH_3 during the exposure time. Increasing diurnal NH_3 variability is associated with an increase in the QCL-EC-to-ALPHA-IHF ratio, indicating that QCL-EC yields higher values relative to ALPHA-IHF under conditions of high variability. Thus, the bias between the methods depends on the magnitude of diurnal NH_3 variability. For every 1 SD increase in diurnal NH_3 variability, the QCL-EC/ALPHA-IHF ratio increases by 31 %. The results also indicate that the relative bias between the two methods further depends on air temperature, turbulence conditions, and ALPHA's profile quality.

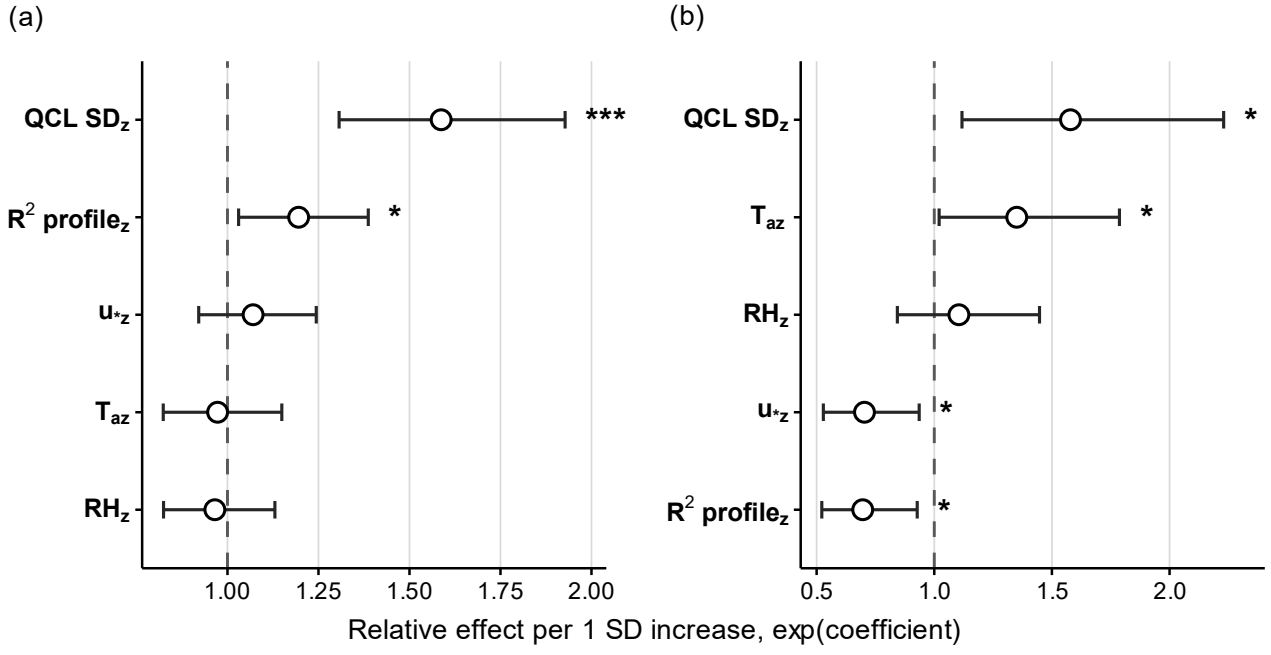

Figure 6: Estimated effects of covariates (QCL SD = variability in atmospheric NH_3 concentration, R^2 profile = ALPHA concentration profile quality, u_* = friction velocity, T_a = air temperature, RH = relative humidity) on the concentration ratio (a), log(QCL/ALPHA), and emission ratio (b), log(QCL-EC/ALPHA-IHF) based on multivariable regression models of the log-transformed ratios. Points represent exponentiated regression coefficients for the standardized (z) covariates, corresponding to a 1 SD increase in each covariate, with horizontal bars indicating 95% confidence intervals. The vertical dashed line at 1 denotes no effect. Values greater than 1 indicate an increase in the respective QCL(-EC)-to-ALPHA(-IHF) ratio, whereas values below 1 indicate a decrease, after adjustment for the other variables included in the model. Significance levels are indicated as follows: * p < 0.05, ** p < 0.01, *** p < 0.001.

https://doi.org/10.5194/egusphere-2026-5494
Preprint. Discussion started: 14 September 2026

In order to evaluate whether there has been an improvement or a deterioration in systematic agreement, the slope must always be considered alongside the current position relative to 0 (Fig. 7). In our data set, the predicted line crosses the zero line for almost all covariates within the observed range of values. This means that the same slope indicates an improvement on one side of the zero line and a deterioration on the other. Points represent partial residuals from the full model, adjusted for mean emission level and all other covariates. Therefore, the plots describe changes in the mean method difference, but not changes in the random scatter of differences between methods.

https://doi.org/10.5194/egusphere-2026-5494
Preprint. Discussion started: 14 September 2026

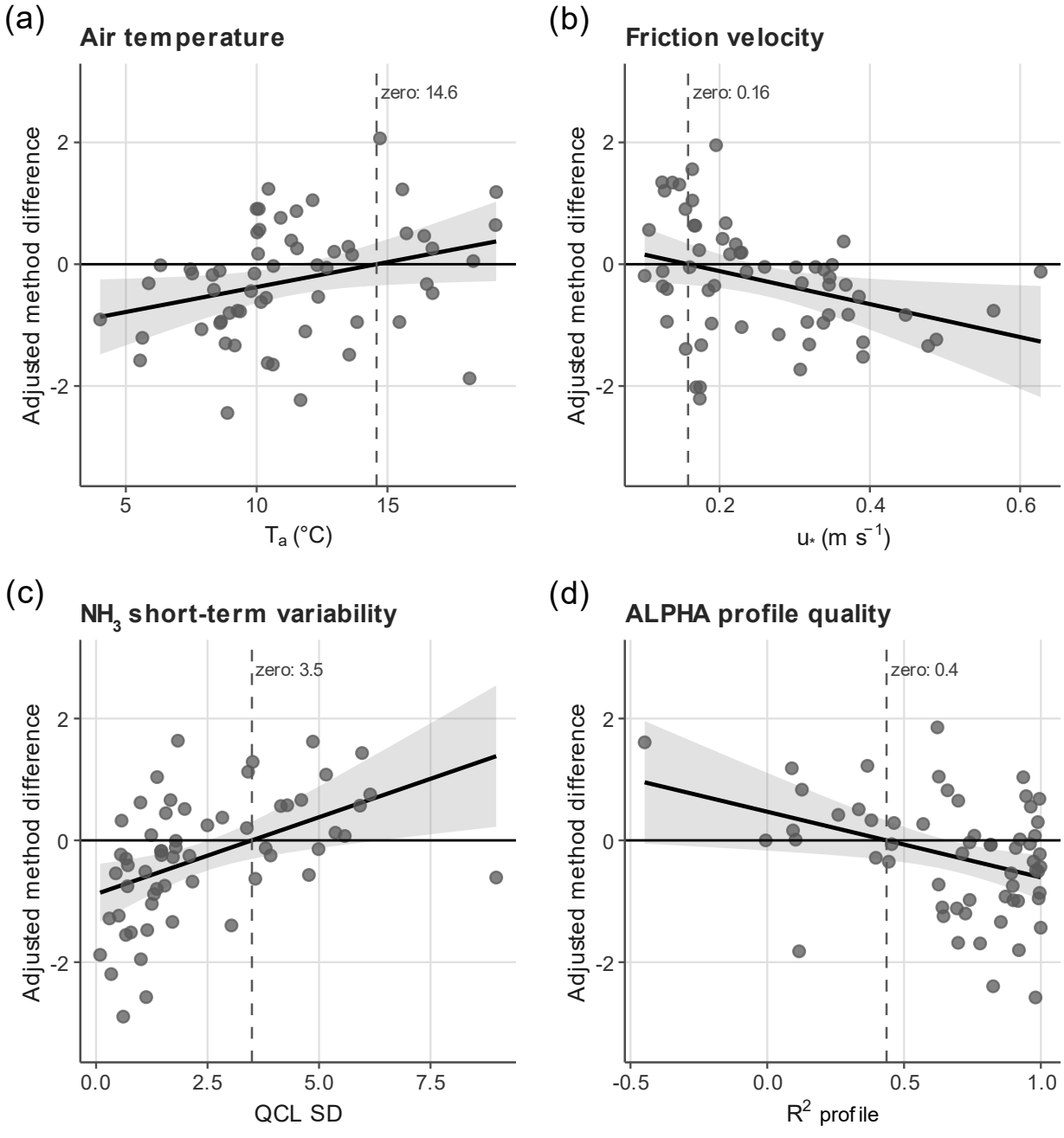

Figure 7: Selected adjusted covariate effect plots for the log ratio between QCL-EC and ALPHA-IHF emission estimates. Points show partial residuals, black lines adjusted linear effects, and grey ribbons 95% confidence intervals. The horizontal zero line indicates equal estimates by both methods; values above zero indicate higher QCL-EC estimates and values below zero lower QCL-EC estimates. Dashed vertical lines mark zero crossings within the observed covariate range.

https://doi.org/10.5194/egusphere-2026-5494
Preprint. Discussion started: 14 September 2026

For example, the two methods show the best systematic agreement at u_* = 0.16 m s^{-1}. As u_* increases further, the QCL-EC method yields progressively lower values than the ALPHA-IHF method (or vice versa), and the two methods therefore diverge. For air temperature, the best agreement is achieved at 14.6 °C: at lower temperatures, QCL-EC yields lower values, whereas at higher temperatures, it yields higher values compared to ALPHA-IHF – however, this does not necessarily mean that QCL-EC emissions increase in absolute terms with temperature. Regarding the NH_3 variability (QCL SD), the best systematic agreement was found at medium diurnal variation (QCL SD = 3.6 µg m^{-3}).

The bivariate model separated the covariate effects into method-specific responses (Fig. 8). For concentrations, ALPHA and QCL showed broadly similar covariate slopes, indicating no clear method-specific sensitivity to the investigated covariates. For emissions, however, method × covariate interactions were more pronounced. ALPHA-IHF showed stronger associations with u_*, profile R^2 and air temperature, whereas QCL-EC fluxes were only weakly associated with these variables. This indicates that the covariate dependence observed in the emission ratio was mainly driven by ALPHA-IHF rather than by QCL-EC.

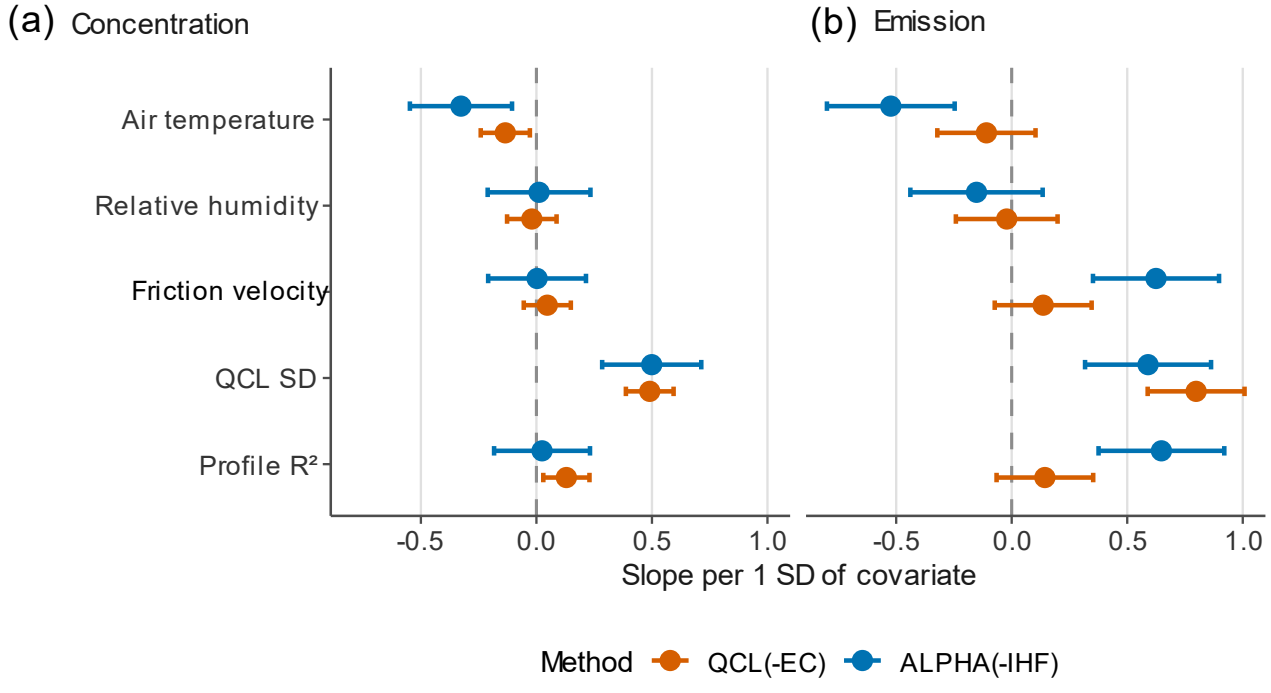

Figure 8: Method-specific covariate slopes from the bivariate model (method × covariate), with 95% confidence intervals, for the concentration (a) and emission (b) endpoints. Each slope is the change in the log reading of one method per 1 SD of the covariate.

https://doi.org/10.5194/egusphere-2026-5494
Preprint. Discussion started: 14 September 2026

4 Discussion

4.1 Temporal dynamics and overall method comparison

A central finding of this study is that QCL-EC and ALPHA-IHF captured similar temporal dynamics but produced only limited quantitative agreement. Changes in NH_3 concentrations and fluxes occurred largely in parallel, and both approaches identified the main emission periods after fertilisation. However, the wide limits of agreement and the differences in cumulative emissions show that agreement in temporal patterns did not translate into close agreement in concentration or emission magnitude. Method-specific error variances indicated unequal precision, while both the magnitude and direction of between-method differences varied with measurement conditions.

The common temporal pattern was broadly consistent with the expected behaviour after urea fertilisation. Following application, urea is hydrolysed by urease, causing a local increase in pH in the fertiliser microsite and shifting the NH_4^+/NH_3 equilibrium towards NH_3. The subsequent partitioning between NH_4^+ and NH_3 and the volatilisation of NH_3 depend on interacting soil and meteorological factors, including soil moisture, temperature, initial soil pH and soil buffering properties (Bouwmeester et al., 1985; Ernst and Massey, 1960; Ferguson et al., 1984; Sommer et al., 2004). In this study, peak emissions occurred on average two to three days after application, and elevated emissions lasted for approximately three days before declining. The main post-application emission activity was therefore concentrated within a relatively short period. However, field studies have shown that emission timing can vary considerably among application dates in response to differences in soil and weather conditions (e.g., Ni et al., 2015). Controlled studies further indicate that low initial soil moisture can delay urea-granule dissolution, while water addition or rainfall can initiate hydrolysis or, when sufficient to transport urea into the soil, reduce NH_3 losses (Sanz-Cobena et al., 2011; Frößl et al., 2025b). Comparisons of emission timing among studies should therefore account for initial soil moisture, subsequent precipitation and fertiliser management.

4.2 Concentration profiles and ALPHA-IHF emission derivation

A central limitation of the ALPHA-IHF approach was that emission estimates could only be derived for 62 % of the investigated periods. For the remaining 38 %, the concentration profiles were physically implausible or showed no sufficiently pronounced and consistent decrease in concentration with height to support robust flux calculation. Consequently, the comparison metrics were based only on periods with valid ALPHA-IHF estimates.

The availability of valid ALPHA-IHF estimates was closely associated with the quality of the fitted concentration profile. Periods with low profile R^2 values were more likely to produce unusable IHF estimates, indicating sensitivity to irregular profiles and to small concentration differences among sampling heights (Fig. 9a). This follows from the conceptual basis of IHF, in which emissions are derived from fitted vertical concentration and wind-speed profiles and their integration over height. Profile selection and specification are therefore critical parts of the calculation. Goedhart et al. (2020) showed that profile misspecification can lead to substantial relative bias and proposed an exponential concentration model with gamma-distributed concentration errors. In this study, we used a modified version of this approach following Kemmann et al. (2025)

https://doi.org/10.5194/egusphere-2026-5494
Preprint. Discussion started: 14 September 2026

that included measured background concentrations and maximum wind speed to reduce the risk of overestimating emissions, particularly under low NH_3 concentrations and strong wind conditions. Nevertheless, this modification remains dataset-specific and required visual inspection and, in some cases, manual decisions about whether a physically meaningful profile could be fitted.

Difficulties in deriving robust ALPHA-IHF estimates occurred particularly towards the end of the campaigns, when concentrations and differences among measurement heights were generally small. The highest NH_3 fluxes occurred mainly during the first part of a campaign, whereas later periods contributed less to cumulative emissions. During these later periods, profiles were often less consistent, as reflected in lower median R^2 values after the first week (Fig. 9b). When the concentration differences among sampling heights and between the source area and background approached the variability of the concentration measurements, small deviations in individual sampler values or background estimates could strongly affect the fitted profile and derived flux.

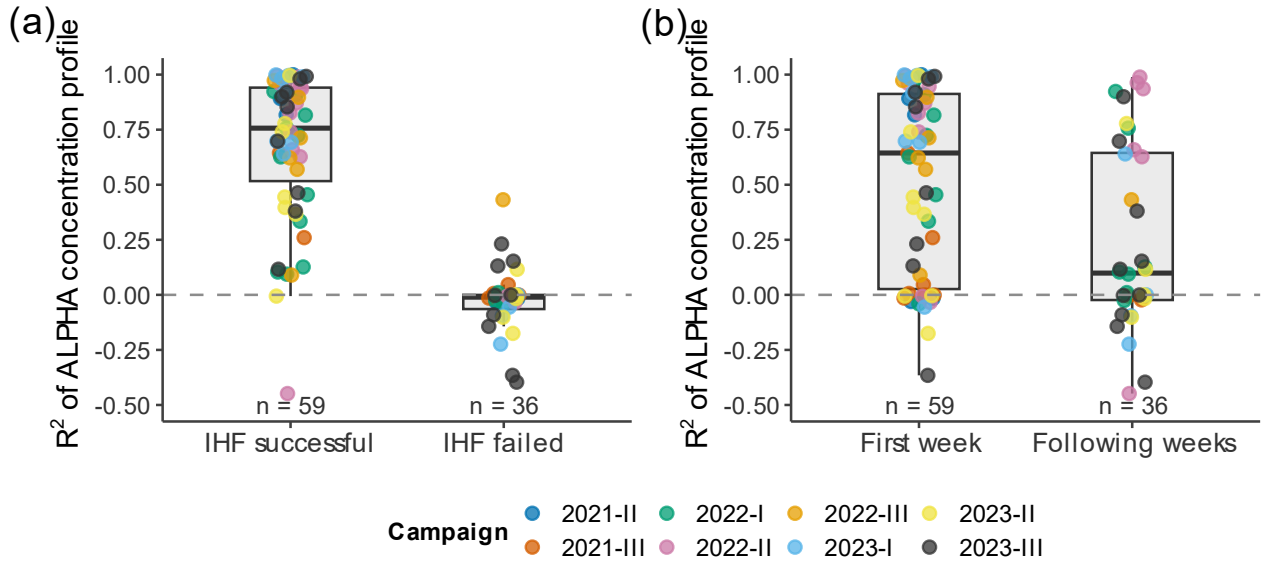

Figure 9: Relationship between (a) the availability of a valid ALPHA-IHF estimate and the coefficient of determination (R^2) of the ALPHA concentration profile and (b) time after fertilisation and profile R^2. Points show individual observations; boxes indicate the median and interquartile range. Missing ALPHA-IHF estimates were classified as method failures. One observation with $R^2 = -1.3$ is outside the displayed y-axis range but was retained in the boxplot calculations.

Whether a different NH_3 sampling system would have increased the availability of valid IHF estimates cannot be determined from this study. Götze et al. (2025) found reasonable agreement between ALPHA- and Leuning-based IHF estimates. However, differences in sampling principle prevent interpreting this comparison as a direct test of sampler precision. Moreover, Kamp et al. (2024) found that active impinger-based IHF could also fail during a later low-emission period when no valid concentration profile could be fitted. These findings do not identify a clearly superior sampler for IHF. A direct

https://doi.org/10.5194/egusphere-2026-5494
Preprint. Discussion started: 14 September 2026

comparison would require alternative concentration systems to be operated simultaneously at identical heights, exposure periods and source conditions while applying the same IHF calculation.

4.3 Comparison of NH_3 concentrations

QCL and ALPHA-derived concentrations were positively related, indicating that both systems captured the temporal variation in NH_3. However, the scatter and wide limits of agreement show substantial differences in individual estimates. On average, QCL concentrations were 31 % higher than ALPHA-derived values, so temporal similarity did not translate into close quantitative agreement.

This mean difference contrasts with previous field intercomparisons, in which the investigated QCL-TILDAS instruments showed overall regression slopes below unity relative to the ensemble mean or median (von Bobrutzki et al., 2010; Twigg et al., 2022). However, these studies compared QCL-TILDAS instruments with heterogeneous instrument ensembles rather than directly with profile-derived ALPHA concentrations. They also reported that instrument agreement varied with concentration range, inlet configuration and instrument setup, with greater relative variability at low concentrations. These studies therefore provide context for the present result but do not explain the observed QCL–ALPHA difference.

Interpretation of this difference must also account for how the matched concentrations were obtained. Although the concentrations were matched by height and averaging period, the QCL concentration was measured directly at 2.5 m, whereas the corresponding ALPHA value was interpolated from the fitted vertical profile. The ALPHA estimate therefore incorporated information from five height-specific triplicate means but also depended on the assumed profile shape and its goodness of fit. Consequently, the comparison encompasses both differences between the concentration measurement techniques and uncertainty introduced by estimating the ALPHA concentration at 2.5 m from the fitted profile.

Potential sources of disagreement occur in both concentration measurement chains. QCL measurements can be affected by inlet configuration and the adsorption and desorption of NH_3 on inlet and tubing surfaces, which can dampen and delay changes in the measured concentration (Ellis et al., 2010; Roscioli et al., 2016; Moravek et al., 2019). For ALPHA, uncertainty can arise from the effective sampling rate, sampler preparation and exposure, extraction and laboratory analysis (Tang et al., 2001). Martin et al. (2019) found particularly good agreement between ALPHA samplers and traceable reference concentrations in controlled-atmosphere tests. However, those tests used substantially longer exposure periods than the height-resolved measurements in the present study and did not include profile fitting. In the present study, the samplers were prepared and handled according to established recommendations, but the contributions of passive sampling, laboratory analysis and profile interpolation could not be separated. The larger error variance associated with the ALPHA-derived concentrations should therefore be attributed to the complete concentration-estimation chain rather than to the ALPHA sampler alone.

The statistical analysis complements these methodological considerations and indicated that the apparent association between the QCL–ALPHA concentration difference and concentration level was largely explained by unequal method-specific error variances. The larger error standard deviation of the ALPHA-derived concentrations indicates lower precision of the complete ALPHA concentration-estimation chain under the conditions of this study. The results therefore support an overall difference

https://doi.org/10.5194/egusphere-2026-5494
Preprint. Discussion started: 14 September 2026

between the methods, but not a pronounced systematic change in agreement across the concentration range. The QCL measurements were more precise, nevertheless, without an independent reference measurement, the observed mean difference cannot be attributed entirely to an underestimation by ALPHA.

4.4 Comparison of NH_3 emissions and derived emission factors

The emission comparison showed a different pattern from the concentration comparison. Although QCL concentrations were 31 % higher on average, QCL-EC emissions were 23 % lower than ALPHA-IHF emissions. This is not inherently contradictory because concentration measurements are only one component of the respective flux calculations. QCL-EC determines the vertical turbulent covariance of NH_3 concentration and vertical wind velocity within the EC footprint. ALPHA-IHF reconstructs the horizontal export of NH_3 from the defined source area using fitted concentration and wind-speed profiles after accounting for background concentrations. Its flux estimate therefore depends on the complete vertical distribution of concentration and wind speed, the background concentration, the integration limits and the assumed source radius. Consequently, a lower concentration at the 2.5-m reference height does not imply a lower IHF flux, because elevated NH_3 concentrations above background at lower heights can contribute substantially to the vertically integrated horizontal flux.

The approaches also represent bidirectional exchange differently. QCL-EC quantifies net turbulent NH_3 exchange above the canopy; deposition may therefore reduce the upward flux even when the resulting half-hourly net flux remains positive. In contrast, the ALPHA-IHF approach estimates positive horizontal export of background-corrected NH_3 from the fertilised source area and does not represent deposition as a negative source strength. This difference may have contributed to the lower QCL-EC emissions, although its magnitude could not be quantified. Canopy recapture of ground-emitted NH_3 can reduce the amount transported above the canopy (Denmead et al., 1976; Denmead et al., 2008; Frößl et al., 2025a). This process may have contributed to the generally low EFs derived by both approaches but is unlikely to fully explain the between-method difference.

Cumulative emissions were also affected by the different treatment of missing periods. Intervals without valid ALPHA-IHF profiles were not gap-filled and therefore did not contribute to cumulative ALPHA-IHF emissions. This could have caused some downward bias, although nearly all such intervals occurred during the later low-emission phase and their contribution was therefore probably small. Conversely, QCL-EC gaps were filled for the calculation of cumulative emissions, introducing uncertainty associated with the gap-filling procedure.

The resulting median emission factors were 1.6 % for QCL-EC and 3.2 % for ALPHA-IHF, both substantially below the IPCC and EMEP default factors for urea of 14.2 % and 16.1 %, respectively. The ALPHA-IHF estimate was below the median but within the range reported by Kemmann et al. (2025) for urea applied to winter wheat in Germany using the same approach (range: 1.1–20.7 %; median: 4.8 %). This comparison is contextual rather than independent because the present site contributed to that multi-site dataset. Direct field studies using QCL-EC-based approaches after urea fertilisation remain scarce (Ferrara et al., 2012; Moravek et al., 2019). Both studies focused primarily on methodological aspects of NH_3 eddy covariance, particularly high-frequency attenuation and quality control, rather than on comprehensive comparisons with independent

https://doi.org/10.5194/egusphere-2026-5494
Preprint. Discussion started: 14 September 2026

cumulative emission estimates. Low fertiliser-related NH_3 losses have also been reported from EC measurements, with Wang et al. (2022) estimating 0.57–0.71% of applied N after compound and organic fertilisation and Vettikkat et al. (2026) reporting 2.25 % of applied TAN following application of separated solid cattle manure, a value at the lower end of the reported range for this fertiliser type. Nevertheless, differences in fertiliser type, EF basis, management, and measurement approach prevent direct quantitative comparison with the present urea-based EFs.

Overall, the difference between methods may partly reflect their different representation of bidirectional exchange and treatment of missing data, while campaign-specific environmental conditions and canopy recapture may additionally help explain the low emission factors obtained with both approaches.

4.5 Methodological aspects of flux estimation

Stably stratified conditions (e.g., during night-time) may further contribute to discrepancies between the two methods and they pose challenges for both approaches. Stable stratification suppresses turbulent vertical mixing, allowing NH_3 to accumulate near the ground rather than being efficiently transported to higher atmospheric layers (cf. Twigg et al., 2022). For QCL-EC, weak or intermittent turbulence may cause flux estimates to fail quality criteria, resulting in gaps that require filling when calculating cumulative emissions. Because ALPHA samplers integrate over the entire exposure period, such near-surface accumulation can strongly influence the resulting concentration profile, which is subsequently combined with exposure-averaged wind speeds for flux calculations. If this near-surface NH_3 accumulation is not temporally coupled with horizontal transport, the integrated concentration profile may overrepresent periods of limited transport, potentially biasing IHF-derived flux estimates. This mechanism is most likely to matter during low-emission periods, when vertical atmospheric NH_3 gradients are relatively weak and small changes in near-surface concentrations can strongly affect the fitted profile. This interpretation is consistent with the observation that ALPHA-IHF became less robust during later low-emission periods, but it remains a hypothesis because storage processes and vertical redistribution were not measured independently.

The different temporal resolution of the two methods is another relevant source of disagreement. ALPHA samplers integrate over several hours or days, whereas QCL provides high-frequency concentration data that were aggregated to the ALPHA exposure period for comparison. Long integration periods can smooth short-term peaks. Conversely, time-integrated samplers may be influenced by periods that contribute strongly to the concentration signal but less strongly to turbulent transport. The importance of temporal variability is supported by the covariate analysis, where the within-period QCL standard deviation explained a substantial part of the systematic variation in the concentration and emission ratios. This suggests that periods with strong NH_3 variability are particularly prone to method differences.

The source area represented another potential source of uncertainty. The circular fertilised plot in our study had a radius of 70 m, which was chosen as a compromise between the requirements of IHF and EC. For IHF, medium-scale circular source plots with radii of 20–50 m are typically used (Sintermann et al., 2012), whereas EC requires a source area that is sufficiently large and homogeneous to represent the flux footprint. A larger source area can therefore be advantageous for EC, but it may increase the uncertainty of the IHF calculation to the representativeness of a single concentration profile and to assumptions

https://doi.org/10.5194/egusphere-2026-5494
Preprint. Discussion started: 14 September 2026

about the effective source area. Previous studies indicate that IHF can provide reasonably accurate emission estimates for uniformly emitting circular source areas. Wilson and Shum (1992) reported deviations of less than approximately 20 % from the prescribed source strength for plot radii exceeding 20 m and surface roughness lengths below 0.1 m. However, conventional IHF calculations based on separately averaged wind speed and concentration neglect horizontal turbulent transport, potentially resulting in a positive bias of approximately 5–20 %, depending on atmospheric stability, plot geometry, and surface roughness (Gao et al., 2009; Sintermann et al., 2012; Wilson and Shum, 1992).

For QCL-EC, method-specific uncertainties are mainly related to the high reactivity of NH_3 and its tendency to adsorb to and desorb from inlet surfaces and tubing. This can dampen fast concentration fluctuations and lead to high-frequency attenuation (Roscioli et al., 2016; Moravek et al., 2019). If not corrected, such damping would lead to an underestimation of EC fluxes. In this study, high-frequency damping correction factors were determined for each half-hour using the co-spectral approach of Wintjen et al. (2020). The mean damping factor was 0.57, corresponding to an estimated flux loss of 43 % before correction, with values ranging from 29 % to 53 %. This magnitude is comparable to high-frequency flux losses reported for closed-path QCL-based NH_3 EC systems (Ferrara et al., 2012; Moravek et al., 2019; Zöll et al., 2016) but it also shows that the correction is a substantial part of the EC flux calculation. Uncertainty in the correction factor therefore directly affects the cumulative QCL-EC emission estimate. Additional EC-related sources of uncertainty include lag-time determination, spectral corrections, footprint mismatch, data filtering, and gap filling (Moravek et al., 2019; Wintjen et al., 2020; Kljun et al., 2015; Lucas-Moffat et al., 2022). These uncertainties do not invalidate the EC approach, but they show that QCL-EC requires extensive post-processing and quality control.

4.6 Influence of measurement conditions

The covariate analyses show that disagreement between the methods was condition dependent and cannot be adequately represented by a single average ratio. For concentrations, covariates alone accounted for little variation, but their contribution became apparent after accounting for the level-dependent pattern in the log-ratio. The remaining associations with within-period NH_3 variability and ALPHA profile quality suggest that the concentration differences were not simply attributable to a constant offset but were also related to temporal integration and the reliability of profile reconstruction. For emissions, the stronger covariate dependence suggests that the conversion of concentration information into flux estimates introduced additional condition sensitivity. Associations with NH_3 variability, air temperature, friction velocity and ALPHA profile quality are consistent with the different responses of turbulence-based EC and profile-based IHF calculations to changing field conditions, although they do not establish causality. Since the fitted log-ratios crossed zero within the observed ranges of several covariates, the method that produced the higher estimate depended on the prevailing conditions. The average between-method difference should therefore not be used as a general correction factor or transferred directly to other campaigns. More broadly, comparisons of NH_3 emission estimates across campaigns or studies must account for differences in measurement conditions and method-specific data coverage, as these may affect the observed between-method differences.

https://doi.org/10.5194/egusphere-2026-5494
Preprint. Discussion started: 14 September 2026

The bivariate model was subsequently used to identify which method contributed most strongly to these patterns and indicated that the observed covariate dependence of the emission ratio was primarily associated with variation in ALPHA-IHF rather than QCL-EC. This is plausible because IHF emissions are reconstructed from concentration and wind-speed profiles and are therefore sensitive to profile shape and profile quality, whereas QCL-EC does not rely on a fitted concentration profile. The stronger covariate response of ALPHA-IHF should therefore be interpreted as condition dependence of the complete IHF calculation chain rather than as evidence of a general systematic bias. This was particularly relevant when concentration differences among ALPHA sampling heights were small relative to the variability in sampler readings and background concentrations, leaving the fitted profile poorly constrained.

4.7 Study limitations and future research

Several limitations should be considered. First, no independent reference method was available, and neither QCL-EC nor ALPHA-IHF can be interpreted as providing the true flux. The study therefore assesses method agreement and method-specific behaviour rather than absolute accuracy. Second, the comparison was based on a single experimental setup without replicated measurement towers, and the source area represented a compromise between the spatial requirements of EC and IHF. Third, cumulative emission estimates from both approaches were subject to method-specific data-availability and processing uncertainties. Invalid ALPHA-IHF intervals were not gap-filled; however, because these occurred almost exclusively during later low-emission phases, their influence on cumulative emissions was likely small, although minor underestimation cannot be excluded. QCL-EC gaps were filled and fluxes were corrected for high-frequency attenuation, making cumulative estimates dependent on these processing steps. The sensitivity of cumulative emissions to these processing steps was not evaluated separately. Fourth, deposition, storage and recapture processes were not quantified independently. Finally, the covariate analyses were exploratory and should be interpreted as indicators of potential mechanisms rather than evidence of causality.

Despite these limitations, the study provides useful methodological insight. Both approaches captured similar temporal emission dynamics but differed in concentration precision, data coverage and condition-dependent performance. ALPHA-IHF is comparatively low-cost and provided field-scale emission estimates when valid concentration and wind profiles could be obtained, but emissions could not be reconstructed for periods without a suitable concentration profile. QCL-EC provided higher-temporal-resolution measurements and greater data coverage, but required technically demanding instrumentation, substantial attenuation correction, quality filtering and gap filling. Neither approach can therefore be considered universally superior.

Future studies should compare alternative active or online multi-height concentration measurements with ALPHA samplers under otherwise identical IHF conditions, particularly during weak-gradient periods, to determine whether profile resolution and data coverage can be improved. For QCL-EC, future work should examine inlet configurations that reduce high-frequency attenuation and quantify the influence of attenuation correction, quality filtering and gap filling on cumulative emissions. Replicated field comparisons or controlled-release experiments could help separate uncertainties in concentration measurement from those arising from the respective flux-calculation approaches.

https://doi.org/10.5194/egusphere-2026-5494
Preprint. Discussion started: 14 September 2026

5 Conclusion

The comparison showed that QCL-EC and ALPHA-IHF captured similar temporal patterns of NH_3 concentrations and emissions after urea fertilisation, but differed in precision, data availability and sensitivity to measurement conditions. ALPHA-IHF provided useful field-scale emission estimates when concentration profiles were well defined, but its applicability was limited under low-emission conditions with weak or irregular concentration gradients. QCL-EC offered high temporal resolution and remained applicable during periods when IHF profiles could not be derived from concentration measurements, but it requires technically demanding and expensive instrumentation, careful quality control and method-specific post-processing. The observed differences between the two approaches cannot be explained by concentration levels alone but instead arise from the complete measurement and flux calculation chains. Ultimately, QCL-EC appears better suited for future applications requiring high sensitivity under low-emission conditions, as the continued development of enhanced-efficiency fertilisers and other emission mitigation strategies will require the quantification of increasingly subtle differences in NH_3 emissions. Such high-sensitivity systems could provide benchmark measurements against which emerging low-cost multi-plot approaches can be evaluated and will be essential for assessing future strategies to mitigate reactive N losses from crop production in agronomic field trials.

Data availability

The data underlying this study are currently being prepared for deposit in a public data repository. Until then, the data are available from the corresponding author upon request.

Supplementary material

The supplementary material provides a detailed description of the statistical analyses and the corresponding R code used to perform them.

Author contributions

Sina Kukowski: Writing – review & editing, Writing – original draft, Visualization, Validation, Methodology, Investigation, Formal analysis, Data curation, Conceptualization, Project administration. **Björn Kemmann:** Writing – review & editing, Investigation, Formal analysis, Validation. **Pascal Wintjen:** Writing – review & editing, Formal analysis, Validation, Methodology, Data curation. **Paul Schmidt:** Writing – review & editing, Formal analysis, Validation, Methodology, Visualization. **Hans-Peter Piepho:** Writing – review & editing, Formal analysis, Methodology, Visualization, Supervision. **Jeremy Rüffer:** Data Curation, Investigation. **Jens-Kristian Jüdt:** Investigation**. Melanie Saul:** Investigation, Resources. **Hannah Götze:** Investigation, Validation. **Andreas Pacholski:** Writing – review & editing, Supervision, Funding acquisition,

https://doi.org/10.5194/egusphere-2026-5494
Preprint. Discussion started: 14 September 2026

Conceptualization. **Heinz Flessa:** Writing – review & editing, Supervision, Funding acquisition, Conceptualization. **Christian Brümmer:** Writing – review & editing, Supervision, Validation, Conceptualization.

Declaration of competing interest

The authors declare that they have no known competing financial interests or personal relationships that could have appeared to influence the work reported in this paper.

Acknowledgments

During the preparation of this work, the authors used Claude (Anthropic) and ChatGPT (OpenAI) to assist with code writing and improve the language and readability of selected passages. After using this tool, the authors reviewed and edited the affected text as needed and take full responsibility for the content of the article.

Financial support

The project was supported by funds of the German Government's Special Purpose Fund held at Landwirtschaftliche Rentenbank [grant number 892976].

References

Bland, J. M. and Altman, D. G.: Measuring agreement in method comparison studies, Stat. Methods Med. Res., 8, 135–160, 1999.

von Bobrutzki, K., Braban, C. F., Famulari, D., Jones, S. K., Blackall, T., Smith, T. E. L., Blom, M., Coe, H., Gallagher, M., Ghalaieny, M., McGillen, M. R., Percival, C. J., Whitehead, J. D., Ellis, R., Murphy, J., Mohacsi, A., Pogany, A., Junninen, H., Rantanen, S., Sutton, M. A., and Nemitz, E.: Field inter-comparison of eleven atmospheric ammonia measurement techniques, Atmos. Meas. Tech., 3, 91–112, https://doi.org/10.5194/amt-3-91-2010, 2010.

Bouwmeester, R. J. B., Vlek, P. L. G., and Stumpe, J. M.: Effect of Environmental Factors on Ammonia Volatilization from a Urea-Fertilized Soil, Soil Sci. Soc. Am. J., 49, 376–381, https://doi.org/10.2136/sssaj1985.03615995004900020021x, 1985.

Bremner, J. M.: Recent research on problems in the use of urea as a nitrogen fertilizer, Fertil. Res., 42, 321–329, https://doi.org/10.1007/BF00750524, 1995.

Brümmer, C., Rüffer, J. J., Delorme, J.-P., Wintjen, P., Schrader, F., Beudert, B., Schaap, M., and Ammann, C.: Reactive nitrogen fluxes over peatland and forest ecosystems using micrometeorological measurement techniques, Earth Syst. Sci. Data, 14, 743–761, https://doi.org/10.5194/essd-14-743-2022, 2022.

Canfield, D. E., Glazer, A. N., and Falkowski, P. G.: The Evolution and Future of Earth's Nitrogen Cycle, Sci. 330, 192–196,

https://doi.org/10.5194/egusphere-2026-5494
Preprint. Discussion started: 14 September 2026

https://doi.org/10.1126/science.1186120, 2010.

Carozzi, M., Loubet, B., Acutis, M., Rana, G., and Ferrara, R. M.: Inverse dispersion modelling highlights the efficiency of slurry injection to reduce ammonia losses by agriculture in the Po Valley (Italy), Agric. For. Meteorol., 171–172, 306–318, https://doi.org/10.1016/j.agrformet.2012.12.012, 2013.

Denmead, O. T.: Micrometeorological methods for measuring gaseous losses of nitrogen in the field, in: Gaseous Loss of Nitrogen from Plant-Soil Systems, edited by: Freney, J. R. and Simpson, J. R., Springer, Dodrecht, 133–157, https://doi.org/10.1007/978-94-017-1662-8_5, 1983.

Denmead, O. T., Freney, J. R., and Simpson, J. R.: A closed ammonia cycle within plant canopy, Soil Biol. Biochem., 8, 161–164, https://doi.org/10.1016/0038-0717(76)90083-3, 1976.

Denmead, O. T., Freney, J. R., and Dunin, F. X.: Gas exchange between plant canopies and the atmosphere: Case-studies for ammonia, Atmos. Environ., 42, 3394–3406, https://doi.org/10.1016/j.atmosenv.2007.01.038, 2008.

DWD: Climate Data Center, Deutscher Wetterdienst, https://opendata.dwd.de/, 2024.

Ellis, R. A., Murphy, J. G., Pattey, E., van Haarlem, R., O'Brien, J. M., and Herndon, S. C.: Characterizing a Quantum Cascade Tunable Infrared Laser Differential Absorption Spectrometer (QC-TILDAS) for measurements of atmospheric ammonia, Atmos. Meas. Tech., 3, 397–406, https://doi.org/10.5194/amt-3-397-2010, 2010.

EMEP/EEA: EMEP/EEA air pollutant emission inventory guidebook 2009: Technical guidance to prepare national emission inventories, EEA Technical Report, European Environment Agency, Copenhagen, https://doi.org/10.2800/23924, 2009.

EMEP/EEA: EMEP/EEA air pollutant emission inventory guidebook 2013: Technical guidance to prepare national emission inventories, EEA Technical Report, European Environment Agency, Copenhagen, https://doi.org/10.2800/92722, 2013.

EMEP/EEA: EMEP/EEA air pollutant emission inventory guidebook 2016: Technical guidance to prepare national emission inventories, EEA Report, European Environment Agency, Copenhagen, https://doi.org/10.2800/247535, 2016.

EMEP/EEA: EMEP/EEA air pollutant emission inventory guidebook 2023: Technical guidance to prepare national air pollutant emission inventories, EMEP-EEA Joint Report, European Environment Agency, Copenhagen, https://doi.org/10.2800/795737, 2023.

Erisman, J. W., Otjes, R., Hensen, A., Jongejan, P., Van Den Bulk, P., Khlystov, A., Möls, H., and Slanina, S.: Instrument development and application in studies and monitoring of ambient ammonia, Atmos. Environ., 35, 1913–1922, https://doi.org/10.1016/S1352-2310(00)00544-6, 2001.

Erisman, J. W., Galloway, J. N., Seitzinger, S., Bleeker, A., Dise, N. B., Petrescu, A. M. R., Leach, A. M., and de Vries, W.: Consequences of human modification of the global nitrogen cycle, Philos. Trans. R. Soc. B Biol. Sci., 368, 20130116, https://doi.org/10.1098/rstb.2013.0116, 2013.

Ernst, J. W. and Massey, H. F.: The Effects of Several Factors on Volatilization of Ammonia Formed from Urea in the Soil, Soil Sci. Soc. Am. J., 24, 87–90, https://doi.org/10.2136/sssaj1960.03615995002400020007x, 1960.

Ferguson, R. B., Kissel, D. E., Koelliker, J. K., and Basel, W.: Ammonia Volatilization from Surface-Applied Urea: Effect of Hydrogen Ion Buffering Capacity, Soil Sci. Soc. Am. J., 48, 578–582,

https://doi.org/10.5194/egusphere-2026-5494
Preprint. Discussion started: 14 September 2026

https://doi.org/10.2136/sssaj1984.03615995004800030022x, 1984.

Ferrara, R. M., Loubet, B., Di Tommasi, P., Bertolini, T., Magliulo, V., Cellier, P., Eugster, W., and Rana, G.: Eddy covariance measurement of ammonia fluxes: Comparison of high frequency correction methodologies, Agric. For. Meteorol., 158–159, 30–42, https://doi.org/10.1016/j.agrformet.2012.02.001, 2012.

Frößl, J., Ruser, R., and Müller, T.: Absorption of 15N Enriched Ammonia by Winter Wheat at Different Growth Stages, J. Plant Nutr. Soil Sci., 188, 171–180, https://doi.org/10.1002/jpln.202300451, 2025a.

Frößl, J., Scholl, M., Hartung, J., Ruser, R., and Müller, T.: How do soil moisture and simulated rainfall drive ammonia emissions after applying inhibited urea fertilizers? – An incubation study, J. Environ. Manage., 376, 124435, https://doi.org/10.1016/j.jenvman.2025.124435, 2025b.

Frößl, J., Brokötter, J., Götze, H., Hartung, J., Heinemann, P., Hofemeister, M., Kelsch, A., Kemmann, B., Malik, W. A., Flessa, H., Kukowski, S., Müller, T., Pacholski, A., and Ruser, R.: Ammonia emissions from inhibited urea fertilizers – Results on mitigation potential and wheat yield from a multisite experiment across six different regions in Germany, Agric. Ecosyst. Environ., 405, 110384, https://doi.org/10.1016/j.agee.2026.110384, 2026.

Gao, Z., Desjardins, R. L., and Flesch, T. K.: Comparison of a simplified micrometeorological mass difference technique and an inverse dispersion technique for estimating methane emissions from small area sources, Agric. For. Meteorol., 149, 891–898, https://doi.org/10.1016/j.agrformet.2008.11.005, 2009.

Genermont, S., Cellier, P., Flura, D., Morvan, T., and Laville, P.: Measuring ammonia fluxes after slurry spreading under actual field conditions, Atmos. Environ., 32, 279—284, 1998.

Goedhart, P. W., Mosquera, J., and Huijsmans, J. F. M.: Estimating ammonia emission after field application of manure by the integrated horizontal flux method: a comparison of concentration and wind speed profiles, Soil Use Manag., 36, 338–350, https://doi.org/10.1111/sum.12564, 2020.

Götze, H., Brokötter, J., Frößl, J., Kelsch, A., Kukowski, S., and Pacholski, A. S.: Assessment of Different Methods to Determine NH3 Emissions from Small Field Plots After Fertilization, Environments, 12, 1–22, https://doi.org/10.3390/environments12080255, 2025.

Govindasamy, P., Muthusamy, S. K., Bagavathiannan, M., Mowrer, J., Jagannadham, P. T. K., Maity, A., Halli, H. M., G. K., S., Vadivel, R., T. K., D., Raj, R., Pooniya, V., Babu, S., Rathore, S. S., L., M., and Tiwari, G.: Nitrogen use efficiency—a key to enhance crop productivity under a changing climate, Front. Plant Sci., 14, 1121073, https://doi.org/10.3389/fpls.2023.1121073, 2023.

Häni, C., Sintermann, J., Kupper, T., Jocher, M., and Neftel, A.: Ammonia emission after slurry application to grassland in Switzerland, Atmos. Environ., 125, 92–99, https://doi.org/10.1016/j.atmosenv.2015.10.069, 2016.

Harper, L. A.: Ammonia: Measurement issues, Micrometeorology Agric. Syst., 345–379, https://doi.org/10.2134/agronmonogr47.c15, 2005.

IPCC: 2019 Refinement to the 2006 IPCC Guidelines for National Greenhouse Gas Inventories, Intergovernmental Panel on Climate Change, Switzerland, 2019.

https://doi.org/10.5194/egusphere-2026-5494
Preprint. Discussion started: 14 September 2026

Irvin, J., Zhou, S., McNicol, G., Lu, F., Liu, V., Fluet-Chouinard, E., Ouyang, Z., Knox, S. H., Lucas-Moffat, A., Trotta, C., Papale, D., Vitale, D., Mammarella, I., Alekseychik, P., Aurela, M., Avati, A., Baldocchi, D., Bansal, S., Bohrer, G., Campbell, D. I., Chen, J., Chu, H., Dalmagro, H. J., Delwiche, K. B., Desai, A. R., Euskirchen, E., Feron, S., Goeckede, M., Heimann, M., Helbig, M., Helfter, C., Hemes, K. S., Hirano, T., Iwata, H., Jurasinski, G., Kalhori, A., Kondrich, A., Lai, D. Y. F., Lohila, A., Malhotra, A., Merbold, L., Mitra, B., Ng, A., Nilsson, M. B., Noormets, A., Peichl, M., Rey-Sanchez, A. C., Richardson, A. D., Runkle, B. R. K., Schäfer, K. V. R., Sonnentag, O., Stuart-Haëntjens, E., Sturtevant, C., Ueyama, M., Valach, A. C., Vargas, R., Vourlitis, G. L., Ward, E. J., Wong, G. X., Zona, D., Alberto, M. C. R., Billesbach, D. P., Celis, G., Dolman, H., Friborg, T., Fuchs, K., Gogo, S., Gondwe, M. J., Goodrich, J. P., Gottschalk, P., Hörtnagl, L., Jacotot, A., Koebsch, F., Kasak, K., Maier, R., Morin, T. H., Nemitz, E., Oechel, W. C., Oikawa, P. Y., Ono, K., Sachs, T., Sakabe, A., Schuur, E. A., Shortt, R., Sullivan, R. C., Szutu, D. J., Tuittila, E.-S., Varlagin, A., Verfaillie, J. G., Wille, C., Windham-Myers, L., Poulter, B., and Jackson, R. B.: Gap-filling eddy covariance methane fluxes: Comparison of machine learning model predictions and uncertainties at FLUXNET-CH4 wetlands, Agric. For. Meteorol., 308–309, 108528, https://doi.org/10.1016/j.agrformet.2021.108528, 2021.

IUSS Working Group WRB: World reference base for soil resources 2014: International soil classification system for naming soils and creating legends for soil maps, 2014.

Kamp, J. N., Hafner, S. D., Huijsmans, J., van Boheemen, K., Götze, H., Pacholski, A., and Pedersen, J.: Comparison of two micrometeorological and three enclosure methods for measuring ammonia emission after slurry application in two field experiments, Agric. For. Meteorol., 354, 110077, https://doi.org/10.1016/j.agrformet.2024.110077, 2024.

Kemmann, B., Brokötter, J., Götze, H., Kelsch, A., Frößl, J., Riesch, S., Heinemann, P., Kukowski, S., Pacholski, A., and Flessa, H.: Ammonia emissions from urea fertilization – Multi-annual micrometeorological measurements across Germany, Agric. Ecosyst. Environ., 381, 109416 Contents, https://doi.org/10.1016/j.agee.2024.109416, 2025.

Kljun, N., Calanca, P., Rotach, M. W., and Schmid, H. P.: A simple parameterisation for flux footprint predictions, Boundary-Layer Meteorol., 112, 503–523, https://doi.org/10.1023/b:boun.0000030653.71031.96, 2004.

Kure, J. L., Krabben, J., Duelund, L., Pedersen, S. V., and Sommer, S. G.: Validation and comparison of ammonia measurement techniques used to determine ammonia absorbed by passive absorption samplers, Can. J. Soil Sci., 100, 175–178, https://doi.org/10.1139/cjss-2019-0124, 2020.

Leuning, R., Freney, J. R., Denmead, O. T., and Simpson, J. R.: A sampler for measuring atmospheric ammonia flux, Atmos. Environ., 19, 1117–1124, https://doi.org/10.1016/0004-6981(85)90196-9, 1985.

Liu, L., Xu, W., Lu, X., Zhong, B., Guo, Y., Lu, X., Zhao, Y., He, W., Wang, S., Zhang, X., Liu, X., and Vitousek, P.: Exploring global changes in agricultural ammonia emissions and their contribution to nitrogen deposition since 1980, Proc. Natl. Acad. Sci. U. S. A., 119, 1–9, https://doi.org/10.1073/pnas.2121998119, 2022.

Lucas-Moffat, A. M., Schrader, F., Herbst, M., and Brümmer, C.: Multiple gap-filling for eddy covariance datasets, Agric. For. Meteorol., 325, 109114, https://doi.org/10.1016/j.agrformet.2022.109114, 2022.

Martin, N. A., Ferracci, V., Cassidy, N., Hook, J., Battersby, R. M., di Meane, E. A., Tang, Y. S., Stephens, A. C. M., Leeson,

https://doi.org/10.5194/egusphere-2026-5494
Preprint. Discussion started: 14 September 2026

S. R., Jones, M. R., Braban, C. F., Gates, L., Hangartner, M., Stoll, J. M., Sacco, P., Pagani, D., Hoffnagle, J. A., and Seitler, E.: Validation of ammonia diffusive and pumped samplers in a controlled atmosphere test facility using traceable Primary Standard Gas Mixtures, Atmos. Environ., 199, 453–462, https://doi.org/10.1016/j.atmosenv.2018.11.038, 2019.

Mauder, M. and Foken, T.: Impact of post-field data processing on eddy covariance flux estimates and energy balance closure, Meteorol. Zeitschrift, 15, 597–609, https://doi.org/10.1127/0941-2948/2006/0167, 2006.

McManus, J. B., Shorter, J. H., Nelson, D. D., Zahniser, M. S., Glenn, D. E., and McGovern, R. M.: Pulsed quantum cascade laser instrument with compact design for rapid , high sensitivity measurements of trace gases in air, Appl. Phys. B – Lasers Opt., 92, 387–392, https://doi.org/10.1007/s00340-008-3129-9, 2008.

Melman, E. A., Wintjen, P., Zhang, J., Rutledge-Jonker, S., Hensen, A., Felter, K., van der Molen, M. K., Snellen, H., de Boer, J., Eijkelboom, M., Haaima, M., van der Hoff, R., van Mansom, H., Voorneveld, J., Vilà-Guerau de Arellano, J., Wichink Kruit, R. J., and van Zanten, M. C.: On the efficiency of biosphere – Atmosphere ammonia exchange processes over a Scots pine forests and its link to ecosystem activity, Agric. For. Meteorol., 389, 111358, https://doi.org/10.1016/j.agrformet.2026.111358, 2026.

Misselbrook, T. H., Nicholson, F. A., Chambers, B. J., and Johnson, R. A.: Measuring ammonia emissions from land applied manure: An intercomparison of commonly used samplers and techniques, Environ. Pollut., 135, 389–397, https://doi.org/10.1016/j.envpol.2004.11.012, 2005.

Moravek, A., Singh, S., Pattey, E., Pelletier, L., and Murphy, J. G.: Measurements and quality control of ammonia eddy covariance fluxes: A new strategy for high-frequency attenuation correction, Atmos. Meas. Tech., 12, 6059–6078, https://doi.org/10.5194/amt-12-6059-2019, 2019.

Ni, K., Köster, J. R., Seidel, A., and Pacholski, A.: Field measurement of ammonia emissions after nitrogen fertilization-A comparison between micrometeorological and chamber methods, Eur. J. Agron., 71, 115–122, https://doi.org/10.1016/j.eja.2015.09.004, 2015.

Oke, T. R.: Boundary Layer Climates, 2 ed. Routledge, London, UK, 1987.

R Core Team: R: A language and environment for statistical computing. R Foundation for Statistical Computing, Vienna, Austria. https://www.R-project.org/, 2021.

Roscioli, J. R., Zahniser, M. S., Nelson, D. D., Herndon, S. C., and Kolb, C. E.: New Approaches to Measuring Sticky Molecules: Improvement of Instrumental Response Times Using Active Passivation, J. Phys. Chem. A, 120, 1347–1357, https://doi.org/10.1021/acs.jpca.5b04395, 2016.

Rothman, L. S., Gordon, I. E., Barbe, A., Benner, D. C., Bernath, P. F., Birk, M., Boudon, V., Brown, L. R., Campargue, A., Champion, J., Chance, K., Coudert, L. H., Dana, V., Devi, V. M., Fally, S., Flaud, J., Gamache, R. R., Goldman, A., Jacquemart, D., Kleiner, I., Lacome, N., Lafferty, W. J., Mandin, J., Massie, S. T., Mikhailenko, S. N., Miller, C. E., Moazzen-ahmadi, N., Naumenko, O. V, Nikitin, A. V, Orphal, J., Perevalov, V. I., Perrin, A., Predoi-cross, A., Rinsland, C. P., Rotger, M., Simeckova, M., Smith, M. A. H., Sung, K., Tashkun, S. A., Tennyson, J., Toth, R. A., Vandaele, A. C., and Vander Auwera, J.: The HITRAN 2008 molecular spectroscopic database, J. Quant. Spectrosc. Radiat. Transf., 110, 533–572,

https://doi.org/10.5194/egusphere-2026-5494
Preprint. Discussion started: 14 September 2026

https://doi.org/10.1016/j.jqsrt.2009.02.013, 2009.

Sanz-Cobena, A., Misselbrook, T., Camp, V., and Vallejo, A.: Effect of water addition and the urease inhibitor NBPT on the abatement of ammonia emission from surface applied urea, Atmos. Environ., 45, 1517–1524, https://doi.org/10.1016/j.atmosenv.2010.12.051, 2011.

Scotto di Perta, E., Fiorentino, N., Carozzi, M., Cervelli, E., and Pindozzi, S.: A Review of Chamber and Micrometeorological Methods to Quantify NH3 Emissions from Fertilisers Field Application, Int. J. Agron., 2020, https://doi.org/10.1155/2020/8909784, 2020.

Sheppard, L. J., Leith, I. A. N. D., Mizunuma, T., and Cape, J. N.: Dry deposition of ammonia gas drives species change faster than wet deposition of ammonium ions: evidence from a long-term field manipulation, Glob. Chang. Biol., 17, 3589–3607, https://doi.org/10.1111/j.1365-2486.2011.02478.x, 2011.

Sintermann, J., Neftel, A., Ammann, C., Häni, C., Hensen, A., Loubet, B., and Flechard, C. R.: Are ammonia emissions from field-applied slurry substantially over-estimated in European emission inventories?, Biogeosciences, 9, 1611–1632, https://doi.org/10.5194/bg-9-1611-2012, 2012.

Skorupka, M. and Nosalewicz, A.: Ammonia volatilization from fertilizer urea—A new challenge for agriculture and industry in view of growing global demand for food and energy crops, Agriculture, 11, https://doi.org/10.3390/agriculture11090822, 2021.

Sommer, S. G. and Misselbrook, T. H.: A review of ammonia emission measured using wind tunnels compared with micrometeorological techniques, Soil Use Manag., 32, 101–108, https://doi.org/10.1111/sum.12209, 2016.

Sommer, S. G., Schjoerring, J. K., and Denmead, O. T.: Ammonia Emission from Mineral Fertilizers and Fertilized Crops, Adv. Agron., 82, 557–622, https://doi.org/10.1016/S0065-2113(03)82008-4, 2004.

Sommer, S. G., McGinn, S. M., and Flesch, T. K.: Simple use of the backwards Lagrangian stochastic dispersion technique for measuring ammonia emission from small field-plots, Eur. J. Agron., 23, 1–7, https://doi.org/10.1016/j.eja.2004.09.001, 2005.

Swart, D., Zhang, J., van der Graaf, S., Rutledge-Jonker, S., Hensen, A., Berkhout, S., Wintjen, P., van der Hoff, R., Haaima, M., Frumau, A., van den Bulk, P., Schulte, R., van Zanten, M., and van Goethem, T.: Field comparison of two novel open-path instruments that measure dry deposition and emission of ammonia using flux-gradient and eddy covariance methods, Atmos. Meas. Tech., 16, 529–546, https://doi.org/10.5194/amt-16-529-2023, 2023.

Tang, Y. S., Cape, J. N., and Sutton, M. A.: Development and types of passive samplers for monitoring atmospheric NO2 and NH3 concentrations, Sci. World J., 1, 513–529, https://doi.org/10.1100/tsw.2001.82, 2001.

Twigg, M. M., Berkhout, A. J. C., Cowan, N., Crunaire, S., Dammers, E., Ebert, V., Gaudion, V., Haaima, M., Häni, C., John, L., Jones, M. R., Kamps, B., Kentisbeer, J., Kupper, T., Leeson, S. R., Leuenberger, D., Lüttschwager, N. O. B., Makkonen, U., Martin, N. A., Missler, D., Mounsor, D., Neftel, A., Nelson, C., Nemitz, E., Oudwater, R., Pascale, C., Petit, J.-E., Pogany, A., Redon, N., Sintermann, J., Stephens, A., Sutton, M. A., Tang, Y. S., Zijlmans, R., Braban, C. F., and Niederhauser, B.: Intercomparison of in situ measurements of ambient NH3: Instrument performance and application under field conditions,

https://doi.org/10.5194/egusphere-2026-5494
Preprint. Discussion started: 14 September 2026

Atmos. Meas. Tech., 15, 6755–6787, https://doi.org/10.5194/amt-15-6755-2022, 2022.

Vettikkat, L., Nissinen, A., Miettinen, P., Jokiniemi, T., Polvinen, T., Koskinen, M., Sirola, M., Pihlatie, M., Virtanen, A., and Schobesberger, S.: Field-scale ammonia flux measurements at an agricultural field in southern Finland by mass spectrometry and eddy covariance, Agric. For. Meteorol., 383, 111121, https://doi.org/10.1016/j.agrformet.2026.111121, 2026.

Vickers, D. and Mahrt, L.: Quality Control and Flux Sampling Problems for Tower and Aircraft Data, J. Atmos. Ocean. Technol., 14, 512–526, 1997.

Wang, K., Kang, P., Lu, Y., Zheng, X., Liu, M., Lin, T., Butterbach-Bahl, K., and Wang, Y.: An open-path ammonia analyzer for eddy covariance flux measurement, Agric. For. Meteorol., 308–309, 108570, https://doi.org/10.1016/j.agrformet.2021.108570, 2021.

Wang, K., Wang, J., Qu, Z., Xu, W., Wang, K., Zhang, H., Shen, J., Kang, P., Zhen, X., Wang, Y., Zheng, X., and Liu, X.: A significant diurnal pattern of ammonia dry deposition to a cropland is detected by an open-path quantum cascade laser-based eddy covariance instrument, Atmos. Environ., 278, 119070, https://doi.org/10.1016/j.atmosenv.2022.119070, 2022.

Whitehead, J. D., Twigg, M., Famulari, D., Nemitz, E., Sutton, M. A., Gallagher, M. W., and Fowler, D.: Evaluation of laser absorption spectroscopic techniques for eddy covariance flux measurements of ammonia, Environ. Sci. Technol., 42, 2041–2046, https://doi.org/10.1021/es071596u, 2008.

Wilczak, J. M., Oncley, S. P., and Stage, S. A.: Sonic anemometer tilt correction algorithms, Boundary-Layer Meteorol., 99, 127–150, 2001.

Wilson, J. D. and Shum, W. K. N.: A re-examination of the integrated horizontal flux method for estimating volatilisation from circular plots, Agric. For. Meteorol., 57, 281–295, https://doi.org/10.1016/0168-1923(92)90124-M, 1992.

Wintjen, P., Ammann, C., Schrader, F., and Brümmer, C.: Correcting high-frequency losses of reactive nitrogen flux measurements, Atmos. Meas. Tech., 13, 2923–2948, https://doi.org/10.5194/amt-13-2923-2020, 2020.

Wyer, K. E., Kelleghan, D. B., Blanes-Vidal, V., Schauberger, G., and Curran, T. P.: Ammonia emissions from agriculture and their contribution to fine particulate matter : A review of implications for human health, J. Environ. Manage., 323, 116285, https://doi.org/10.1016/j.jenvman.2022.116285, 2022.

Yang, W., Que, H., Wang, S., Zhu, A., Zhang, Y., He, Y., Xin, X., and Zhang, X.: Comparison of backward Lagrangian stochastic model with micrometeorological mass balance method for measuring ammonia emissions from rice field, Atmos. Environ., 211, 268–273, https://doi.org/10.1016/j.atmosenv.2019.05.028, 2019.

Zahniser, M. S., Nelson, D. D., Mcmanus, J. B., Shorter, J. H., Herndon, S., and Jimenez, R.: Development of a Quantum Cascade Laser-Based Detector for Ammonia and Nitric Acid, 1409 pp., 2005.

Zöll, U., Brümmer, C., Schrader, F., Ammann, C., Ibrom, A., Flechard, C. R., Nelson, D. D., Zahniser, M., and Kutsch, W. L.: Surface-atmosphere exchange of ammonia over peatland using QCL-based eddy-covariance measurements and inferential modeling, Atmos. Chem. Phys., 16, 11283–11299, https://doi.org/10.5194/acp-16-11283-2016, 2016.